

Deformation of Matrix Geometry via Landau Level Evolution

Kazuki Hasebe

National Institute of Technology, Sendai College, Ayashi, Sendai, 989-3128, Japan
Department of Physics, University of Hong Kong, Pokfulam Road, Hong Kong, China

khasebe@sendai-nct.ac.jp
hasebe@hku.hk

October 22, 2024

Abstract

We propose a scheme for the construction of deformed matrix geometries using Landau models. The level projection method cannot be applied straightforwardly to extract matrix geometries to the Landau models on deformed manifolds, as they do not generally exhibit degenerate energy levels (Landau levels). We overcome this problem by exploiting the idea of spectral flow. Taking a symmetric matrix geometry as a reference point of the spectral flow, we evolve the matrix geometry by deforming the Landau model. In this process, unitarity is automatically preserved. The explicit matrix realization of the coordinates is derived straightforwardly even for a non-perturbative deformation. We clarify the basic properties of the matrix geometries through the analysis of concrete models. The matrix geometries of an expanding two-sphere and ellipsoids are investigated using the non-relativistic and relativistic Landau models. The obtained ellipsoidal matrix geometries show behaviors quantitatively different in each Landau level, but qualitatively similar to their classical counterpart. The difference between the ellipsoidal matrix geometry and the fuzzy ellipsoid is investigated numerically.

Contents

1	Introduction	2
2	Prescription for the deformation of matrix geometry	3
2.1	Matrix geometry for G/H	3
2.2	Matrix geometry deformation via the spectral flow	3
2.3	Matrix geometry evolution and unitarity	5
3	Matrix geometry of the fuzzy sphere	6
3.1	Classical algebra of sphere-coordinates	6
3.2	$SO(3)$ Landau model and the fuzzy two-sphere	6
3.3	Expanding fuzzy sphere	9
4	Classical ellipsoidal geometry and magnetic field	10
4.1	Geometric quantities	10
4.2	Classical algebra of ellipsoid-coordinates	12
4.3	Gauge field and magnetic field	13
5	Non-relativistic Landau model and matrix geometries	15
5.1	Symmetry and eigenvalue problem on an ellipsoid	15
5.2	Evolution of the Landau levels and matrix geometries	16
6	Relativistic Landau models on the ellipsoid	20
6.1	Dirac-Landau operator	20
6.2	Supersymmetric Landau model	21
6.3	Zero-modes and the Atiyah-Singer index theorem	23
7	Ellipsoidal matrix geometry and fuzzy ellipsoid	24
7.1	Ellipsoidal matrix geometries	24
7.2	Comparison to the fuzzy ellipsoid	26
8	Summary	28
A	Riemannian geometry of ellipsoid	29
B	Free particle on an ellipsoid	30
B.1	Non-relativistic free particle on an ellipsoid	30
B.2	Relativistic free particle on an ellipsoid	30

1 Introduction

Non-commutative geometry is a mathematical framework for describing quantum space-time and is still a framework in progress, where many interesting ideas and the methods are being born and applied. The idea of non-commutative geometry is important in many branches of physics, not only in particle physics [1, 2, 3, 4, 5] but also in condensed matter physics [6, 7, 8, 9, 10, 11, 12, 13, 14, 15], quantum information [16, 17], and CFT [18, 19, 20, 21]. One of the best known examples is the fuzzy sphere [22, 23], which realizes a classical solution of Matrix models and the Landau level geometry. Since the late 90s, the researches on the constructions of fuzzy manifolds have progressed rapidly. In this development, fuzzy manifolds corresponding to symmetric manifolds are constructed, such as fuzzy $\mathbb{C}P^n$ [24, 25], higher dimensional fuzzy spheres [26, 27, 28, 29], fuzzy hyperboloids [30, 31] and their supersymmetric versions [32, 33, 34]. Their geometries were realized in the context of the Landau models, as for $\mathbb{C}P^n$ [35, 36], S^n [37, 38, 39, 40, 41, 42, 43, 44, 45], their supersymmetric versions [46, 47] and T^n [48, 49].

Having established the fuzzification of such symmetric manifolds, an important next direction is to consider the fuzzification of the manifolds with less or no symmetries. There have been several early works already in this direction. To the best of author's knowledge, the fuzzification of the 2D Riemannian surfaces with multiple genus has been investigated in Refs.[50, 51] based on some deformed algebra. For mathematical aspects of the classical geometry and its quantization, the readers may consult with Refs.[52, 53, 54, 55]. Another important direction will be the time evolution of fuzzy spaces. An expanding fuzzy sphere has been analyzed in Refs.[56, 57], where the matrix size of the fuzzy space is changed under the evolution and the evolution is non-unitary. An expanding universe is studied recently also in the context of the IKKT matrix model [58, 59]. The semi-classical analysis of the evolving non-commutative spacetime has been performed in [60, 61] and [62] based on the non-compact fuzzy spaces [31]. While the deformed fuzzy geometry and the time evolution of the fuzzy geometry are different in a strict sense, they are closely related in the sense that the evolution usually involves the deformation of space.

In this work, we propose a scheme to construct non-symmetric matrix geometries in the perspective of the evolution of matrix geometries. Recently, the author proposed to generate matrix geometries using the Landau models [45, 37].¹ Interestingly, it was shown that the higher Landau levels exhibits unique matrix geometries distinct from that of the lowest Landau level [45]. We combine this new scheme with the idea of spectral flow to derive deformed matrix geometries. We use a symmetric matrix geometry as a reference point from which the spectral flow starts and trace the evolution of the matrix geometry from it to a non-symmetric manifold of interest through the spectral flow. This method naturally realizes the deformation of non-commutative space associated with the time evolution. While this scheme is very simple and intuitive, it has several unique advantages. First, the derivation of the matrix coordinates, which are very important in practical applications, is straightforward. In the former approaches based on deformed algebras, the concrete matrix realizations to satisfy the deformed algebra are generally difficult to find. Second, since the spectral flow is a concept irrelevant to perturbation, we can discuss non-perturbative deformations of the matrix geometries. Last, since we trace the evolution of the states by the spectral flow, the unitarity of the non-commutative space is automatically guaranteed (without resorting to "exotic" scenarios such as multi-universe [56]). To demonstrate this scheme, we consider two evolutions of the fuzzy two-sphere. The first is the expanding fuzzy sphere, which keeps the $SU(2)$ symmetry along the evolution. The other is the deformation to an ellipsoidal matrix geometry. In this process, the $SU(2)$ symmetry is no longer guaranteed and the Landau level degeneracy is lifted. The spectral flux is therefore essential for tracing the deformation from fuzzy sphere to ellipsoidal matrix geometry.

The paper is organized as follows. In Sec.2, we present the idea of the deformation of matrix geometries

¹The Boerezin-Toeplitz quantization, which have been successfully applied to the matrix geometries [42, 63, 48, 65], corresponds to the zeroth Landau level projection. In this sense, the present method includes the Berezin-Toeplitz quantization as a special case.

using the spectral flow. In Sec.3, we review the fuzzy sphere obtained from the Landau level projection. The matrix geometry of the expanding sphere is discussed. Sec.4 presents the classical geometry and the algebra on the ellipsoid. We introduce a gauge field to be compatible with the geometry of the ellipsoid. In Sec.5, we numerically solve the non-relativistic Landau problem on the ellipsoid and derive the spectral flow with respect to the deformation from sphere to ellipsoid. The corresponding matrix geometries are derived. Their relativistic versions are investigated in Sec.6. In Sec.7, we numerically analyze basic features of the ellipsoidal matrix geometries in comparison with their commutative counterparts and the fuzzy ellipsoids. Sec.8 is devoted to summary and discussion.

2 Prescription for the deformation of matrix geometry

In this section, we propose a scheme for the deformation of matrix geometries from the perspective of the spectral flow.

2.1 Matrix geometry for G/H

To generate the matrix geometry of $\mathcal{M} \simeq G/H$, we use the Landau model with gauge symmetry H on \mathcal{M} [45]. We apply the level projection to a Landau level to extract the matrix geometry:

$$(X_i)_{mn} = \langle \psi_m | x_i | \psi_n \rangle, \quad (2.1)$$

where $|\psi_m\rangle$ denote the degenerate Landau level eigenstates. The size of the matrix coordinates X_i is equal to the degeneracy of the Landau level. This scheme is practically useful to derive the explicit form of the matrix coordinates. When applying the procedure to the Landau models on non-symmetric manifolds, we however immediately find a difficulty. Since the energy levels of the Landau model on a non-symmetric manifold do *not* accommodate degeneracies in general, we simply do not know how to identify the energy levels to which the level projection is applied.

2.2 Matrix geometry deformation via the spectral flow

Any non-symmetric manifold can be obtained from a continuous deformation of a symmetric manifold (with the same topology). We extend this basic picture to derive non-symmetric matrix geometry. To translate this classical picture in the language of quantum mechanics, we consider two Landau models on a symmetric manifold and a non-symmetric manifold of interest. We introduce a deformation parameter μ to connect these two manifolds.² We construct a parameter dependent Hamiltonian $H^{(\mu)}$ that interpolates the two Landau Hamiltonians on the symmetric manifold and the non-symmetric manifold. Take $\mu = \mu_{\text{ini}}$ for an initial symmetric manifold and another value μ_{fin} for the final non-symmetric manifold. The Landau Hamiltonian on the symmetric manifold is denoted by $H^{(\mu_{\text{ini}})}$, and its eigenvalues $E^{(\mu_{\text{ini}})}$ signify the Landau level with degeneracy. Similarly, we denote the Landau Hamiltonian on the non-symmetric manifold as $H^{(\mu_{\text{fin}})}$ and its eigenvalues as $E^{(\mu_{\text{fin}})}$, which are no longer degenerate in general. We then solve the eigenvalue problem of the parameter dependent Hamiltonian,

$$H^{(\mu)}\psi^{(\mu)} = E^{(\mu)}\psi^{(\mu)}. \quad (2.2)$$

Here, $E^{(\mu)}$ signifies the spectral flow of the eigenenergies from $E^{(\mu_{\text{ini}})}$ to $E^{(\mu_{\text{fin}})}$ (the up of Fig.1). Since the energy eigenstates are associated with the energy eigenvalues, it is also possible to trace the evolution of the eigenstates from $\psi^{(\mu_{\text{ini}})}$ to $\psi^{(\mu_{\text{fin}})}$ by tracing the spectral flow. In this way, we can identify the

² μ can be a set of parameters.

eigenstates on the non-symmetric manifold needed for the level projection in (2.1). Since the degrees of freedom do not increase or decrease in the process of spectral flow, the unitarity of the non-commutative spaces is guaranteed. Also note that the spectral flow itself is a concept irrelevant to perturbation and we can discuss non-perturbative deformation of the matrix geometry.

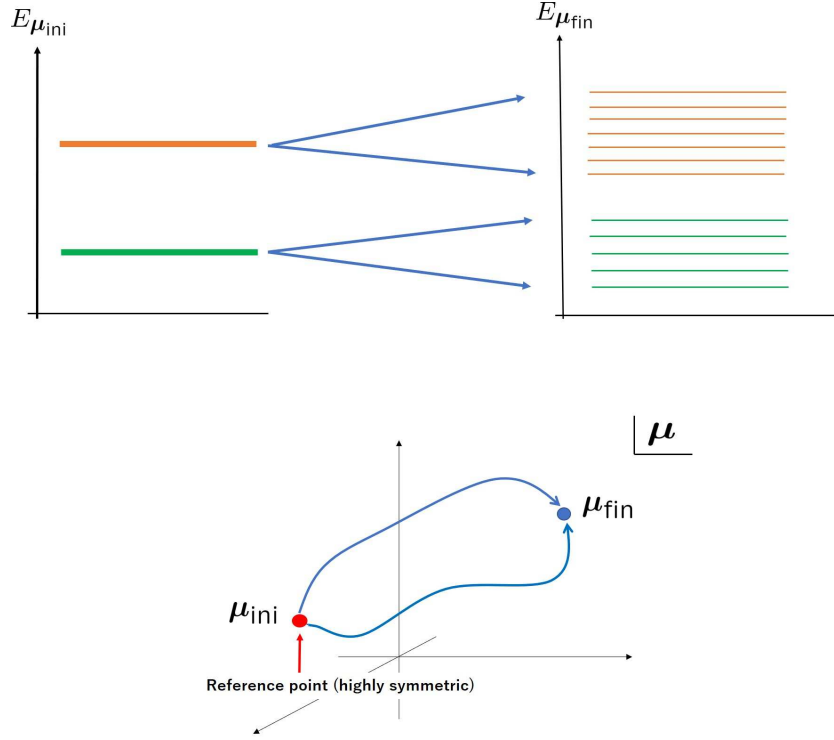


Figure 1: Evolution of the Landau levels. Up: The degeneracy of the Landau level on a symmetric manifold (left) is lifted through the deformation to be a deformed manifold of interest (right). Down: There are an infinite number of paths that connect the initial value of the deformation parameter and the final value in the parameter space. (In the figure, only two paths are depicted.)

As there are an infinite number of paths that connect μ_{ini} and μ_{fin} (the down of Fig.1), careful readers may wonder whether the evolved eigenstates can depend on the choice of the path and the matrix coordinates also. Obviously, the energy spectrum of the deformed manifold does not depend on the path, however, the phases of the eigenstates do depend on the path which they undergo. Consequently, the explicit form of the matrix coordinates obtained by the formula (2.1) generally depends on the path chosen, but the difference of the eigenstates are only their phases.³ Therefore, the two matrix coordinates corresponding to different paths are related by a unitary transformation. In other words, the algebraic relations of these matrix coordinates are unitarily equivalent, and so the algebraic structure of the matrix geometry is independent of the choice of path. The choice of path thus does not affect the algebraic structure of the matrix geometry.

³If the energy levels are degenerate, the (geometric) phase is not simply $U(1)$, but a Wilczek-Zee non-Abelian phase. Then, the difference of the eigenstates is accounted for by a unitary transformation.

2.3 Matrix geometry evolution and unitarity

We further parameterize the path $\boldsymbol{\mu}$ with the parameter t as

$$\boldsymbol{\mu} = \boldsymbol{\mu}(t). \quad (\boldsymbol{\mu}_{\text{ini}} := \boldsymbol{\mu}(t=0)) \quad (2.3)$$

The matrix coordinates are given by

$$X_i(t) = P_N(t)x_iP_N(t), \quad (2.4)$$

where $P_N(t)$ denotes the projection operator onto the subspace of the eigenstates evolving from the N th Landau level with degeneracy d_N :

$$P_N(t) := \sum_{n=1}^{d_N} |\psi_n(t)\rangle\langle\psi_n(t)|. \quad (2.5)$$

Assuming that t represents the time parameter, the evolution of the state can be regarded as the time evolution of the state-vector determined by the time-dependent Schrödinger equation:

$$i\frac{d}{dt}|\psi_n(t)\rangle = H(t)|\psi_n(t)\rangle. \quad (2.6)$$

At $t = 0$, $|\psi_n(0)\rangle$ denote the degenerate Landau level eigenstates:

$$H(0)|\psi_n(0)\rangle = E_N|\psi_n(0)\rangle \quad (n = 1, 2, \dots, d_N). \quad (2.7)$$

For $t \neq 0$, the Landau level degeneracy is generally lifted, and $|\psi_n(t)\rangle$ become the eigenstates of different energy levels. From (2.6), we can see that $P_N(t)$ satisfies

$$\frac{d}{dt}P_N(t) = i[P_N(t), H(t)]. \quad (2.8)$$

A straightforward calculation tells⁴

$$\frac{dX_i(t)}{dt} - i[X_i(t), H(t)] = P_N(t) \left(\frac{dx_i(t)}{dt} - i[x_i(t), H(t)] \right) P_N(t). \quad (2.11)$$

Eq.(2.11) signifies the relation between the evolution of the matrix geometry and that of the classical geometry. We can derive the evolution of the matrix coordinates by solving the differential equation (2.11) with given $H(t)$, $P_N(t)$ and $x_i(t)$. Note that $\frac{d}{dt}X_i$ is not simply equal to the projection of $\frac{d}{dt}x_i$ ($\frac{dX_i(t)}{dt} \neq P_N(t)\frac{dx_i(t)}{dt}P_N(t)$). In the case $P_N = 1$, X_i is equal to x_i , and Eq.(2.11) becomes a trivial equation. While Eq.(2.11) determines the evolution of the matrix coordinates, it is practical to use the following formula to trace the evolution of the matrix geometry,

$$(X_i(t))_{mn} = \langle\psi_m(t)|x_i(t)|\psi_n(t)\rangle. \quad (2.12)$$

Since we follow the unitary-evolution of the state-vector, the unitarity of the time evolution of non-commutative space is *necessarily* guaranteed.

⁴Using the coordinates in the Heisenberg picture $h_i := U(t)^\dagger x_i(t)U(t)$ ($U(t) := \text{Te}^{-i\int_0^t ds H(s)}$) and the Heisenberg equations of motion

$$\frac{d}{dt}h_i(t) = U(t)^\dagger \left(\frac{dx_i(t)}{dt} - i[x_i(t), H(t)] \right) U(t), \quad (2.9)$$

(2.11) can be concisely represented as

$$\frac{dX_i(t)}{dt} - i[X_i(t), H(t)] = P_N(t)U(t)\frac{dh_i(t)}{dt}U(t)^\dagger P_N(t). \quad (2.10)$$

3 Matrix geometry of the fuzzy sphere

In this section, we give a brief review of the fuzzy two-sphere that emerges in the $SO(3)$ Landau model. We also discuss the expanding fuzzy sphere to see how the present scheme works.

3.1 Classical algebra of sphere-coordinates

Let us start with the classical algebra on a two-sphere. Two-sphere is homeomorphic to $\mathbb{C}P^1$, which is a Kähler manifold with Kähler form

$$K = i \frac{2}{(1 + |z|^2)^2} dz \wedge d\bar{z}. \quad (3.1)$$

The complex coordinate z is known as the inhomogeneous coordinate of $\mathbb{C}P^1$. We can parameterize z as

$$z = \tan\left(\frac{\theta}{2}\right) e^{i\phi}. \quad (3.2)$$

With the coordinates on S^2

$$x_1 = \sin \theta \cos \phi, \quad x_2 = \sin \theta \sin \phi, \quad x_3 = \cos \theta, \quad (3.3)$$

we see that the inhomogeneous coordinate z (3.2) is equal to the stereographic coordinates on $\mathbb{C} \simeq \mathbb{R}^2$:

$$z = \frac{1}{1 + x_3} (x_1 + ix_2). \quad (3.4)$$

The Kähler form (3.1) is expressed as

$$K = \sin \theta \, d\theta \wedge d\phi, \quad (3.5)$$

which has a clear geometric meaning, the area element of S^2 . Regarding the Kähler form as a symplectic form, we consider the Kähler manifold as a symplectic manifold and rewrite (3.5) as the canonical form, $K = d\zeta \wedge d\phi$, where ζ and ϕ are the Darboux coordinates (canonical coordinates),

$$\zeta := \int d\theta \sin \theta = -\cos \theta. \quad (3.6)$$

Using (3.5), we can represent the Poisson bracket on the S^2 as

$$\{f, g\} = \frac{\partial f}{\partial \zeta} \frac{\partial g}{\partial \phi} - \frac{\partial f}{\partial \phi} \frac{\partial g}{\partial \zeta} = \frac{1}{\sin \theta} \left(\frac{\partial f}{\partial \theta} \frac{\partial g}{\partial \phi} - \frac{\partial f}{\partial \phi} \frac{\partial g}{\partial \theta} \right). \quad (3.7)$$

Substituting (3.3) to (3.7), we can easily derive the classical algebra of the sphere-coordinates:

$$\{x_i, x_j\} = \sum_{k=1}^3 \epsilon_{ijk} x_k \quad \left(\sum_{i=1}^3 x_i x_i = 1 \right). \quad (3.8)$$

3.2 $SO(3)$ Landau model and the fuzzy two-sphere

Next, we discuss a quantum mechanical counterpart of (3.8) following to [37]. On a sphere with unit radius, the $SO(3)$ Landau Hamiltonian is given by [66, 67]

$$H = -\frac{1}{2M} \sum_{i=1}^3 (\partial_i + iA_i)^2|_{r=1} = \frac{1}{2M} \sum_{i=1}^3 \Lambda_i^2 = -\frac{1}{2M} \left(\partial_\theta^2 + \cot \theta \partial_\theta + \frac{1}{\sin^2 \theta} (\partial_\phi + iA_\phi)^2 \right) \quad (3.9)$$

where

$$\Lambda_i = -i \sum_{k=1}^3 \epsilon_{ijk} x_j (\partial_k + iA_k). \quad (3.10)$$

In the following, we adopt the Schwinger gauge⁵, where the gauge field and the field strength are represented as

$$A = -\frac{I}{2} \cos \theta d\phi, \quad F = dA = \frac{I}{2} \sin \theta d\theta \wedge d\phi = \frac{1}{2} \epsilon_{ijk} B_k dx_i \wedge dx_j \quad (3.11)$$

with

$$B_i = \frac{I}{2r^3} x_i. \quad (3.12)$$

Here I denotes a quantized monopole charge and is taken to be a positive integer henceforth. In the Schwinger gauge, the direction of the gauge field is opposite in the north and south hemi-spheres, $A_\phi(\theta) = -\frac{I}{2} \cos \theta = -A_\phi(\pi - \theta)$. In other words, the gauge field has the mirror symmetry with respect to $z = 0$. The magnetic field is perpendicular to the surface of the two-sphere and the configuration of the magnetic field respects the $SO(3)$ symmetry. The gauge field configuration is thus compatible with the geometry of the base-manifold S^2 . The Hamiltonian then respects the $SO(3)$ symmetry generated by the angular momentum operators

$$[H, L_i] = 0, \quad (3.13)$$

with

$$L_i := \Lambda_i + r^2 B_i, \quad (3.14)$$

which satisfy the $su(2)$ algebra

$$[L_i, L_j] = i \sum_{k=1}^3 \epsilon_{ijk} L_k. \quad (3.15)$$

Using a group theoretical method, it is not difficult to obtain the eigenvalues of H (3.9) as

$$E_N = \frac{1}{2M} (N(N+1) + I(N + \frac{1}{2})), \quad (3.16)$$

where $N(= 0, 1, 2, 3, \dots)$ denotes the Landau level index. The degeneracy of the N th Landau level is given by $2N + I + 1$. The degenerate Landau level eigenstates are known as the monopole harmonics $Y_{N,m}(\theta, \phi)$ with m being the quantum magnetic number:

$$m = N + \frac{I}{2}, N + \frac{I}{2} - 1, \dots, -N - \frac{I}{2}. \quad (3.17)$$

The monopole harmonics are normalized as $\int_{S^2} d\theta d\phi \sin \theta Y_{N,m}(\theta, \phi)^* Y_{N',m'}(\theta, \phi) = \delta_{NN'} \delta_{mm'}$. From the formula (2.1), the matrix coordinates in N th Landau level are derived as [37]

$$(X_i)_{mn} := \int_{S^2} d\theta d\phi \sin \theta Y_{N,m}(\theta, \phi)^* x_i Y_{N,n}(\theta, \phi) = \alpha(I, N) (S_i^{(\frac{I}{2}+N)})_{mn}. \quad (3.18)$$

where

$$\alpha(I, N) := \frac{2I}{(I + 2N)(I + 2N + 2)}. \quad (3.19)$$

The parameter $\alpha(I, N)$ is referred to as the non-commutative scale that describes the spacing between the adjacent states on the fuzzy sphere (see the left of Fig.2). The matrix size of X_i is equal to the Landau

⁵See Ref.[37] for instance.

level degeneracy, $2N + I + 1$. The coordinates are effectively represented by the $su(2)$ matrices with the $SU(2)$ spin index $J = \frac{I}{2} + N$ and satisfy

$$\sum_{i=1}^3 X_i X_i = r(I, N)^2 \mathbf{1}_{I+2N+1}, \quad [X_i, X_j] = i\alpha(I, N) \sum_{k=1}^3 \epsilon_{ijk} X_k, \quad (3.20)$$

where

$$r(I, N) := \alpha(I, N) \cdot \frac{\sqrt{(I+2N)(I+2N+2)}}{2} = \frac{I}{\sqrt{(I+2N)(I+2N+2)}}. \quad (3.21)$$

Note that (3.20) realizes a natural quantum counterpart of the classical relation (3.8). Thus, the geometry of the fuzzy sphere emerges in *any* Landau level. The second relation of (3.20) implies that the matrix coordinates act as the generators of the $SU(2)$ rotations for the fuzzy two-sphere. The fuzzy sphere obviously has the $SU(2)$ symmetry

$$[\mathbf{X}^2, X_i] = 0, \quad (3.22)$$

which is a consequence of the $SO(3)$ symmetry of the original Landau model. Since three X_i s are not commutative, there is no concept of definite points for the fuzzy sphere due to the uncertainly relation of the coordinates. Three matrix coordinates are not simultaneously diagonalized, but only one of X_i is diagonalized to represent the “points” on the fuzzy sphere. We take this matrix coordinate as X_3 , whose eigenvalues represent the positions of the latitudes as shown in the left of Fig.2. In other words, the latitudes, which are spaced by the non-commutative scale α , denote the “points” constituting the fuzzy sphere. The right of Fig.2 represents the absolute values of the lowest Landau level eigenstates (the monopole harmonics of $N = 0$). Obviously, there is one to one correspondence between the constituent “points” of the matrix geometry and the Landau level eigenstates. Thus the fuzzy sphere can be seen as a set of degenerate eigenstates of Landau level.

The continuum limit corresponds to $I \rightarrow \infty$ in which the non-commutative scale (3.19) goes to zero $\alpha(I, N) \rightarrow 0$. Indeed, in this limit, the first equation of (3.20) is reduced to the definition of the unit-radius continuum sphere and the right hand of the second equation of (3.20) vanishes, meaning that X_i are regarded as commutative coordinates.

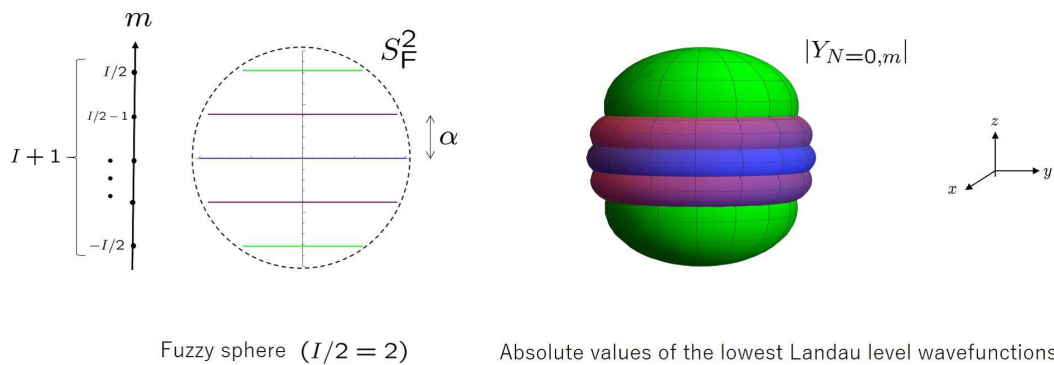


Figure 2: Left: The matrix geometry of the fuzzy sphere (the dashed circle is added as a guide for the eyes). The eigenvalues of X_3/α are plotted on the m -axis. The lengths of the latitudes correspond the eigenvalues of $2\sqrt{X^2 + Y^2}$. Right: The distributions of the absolute values of the monopole harmonics for $m = \pm 2$ (green), ± 1 (purple), and 0 (blue).

For the relativistic Landau model, the fuzzy spheres emerge again as the matrix geometry in each

Landau level [37]. In particular, the matrix coordinates in the zeroth Landau level are given by

$$X_i = \alpha(I-1) S_i^{(\frac{I}{2}-\frac{1}{2})} \left(\alpha(I-1) := \alpha(I-1, N=0) = \frac{2}{I+1} \right), \quad (3.23)$$

which satisfy

$$\sum_{i=1}^3 X_i X_i = \frac{I-1}{I+1} \mathbf{1}_I, \quad [X_i, X_j] = i\alpha(I-1) \sum_{k=1}^3 \epsilon_{ijk} X_k. \quad (3.24)$$

3.3 Expanding fuzzy sphere

To see how the present scheme works, we consider an expansion of the fuzzy two-sphere. The classical two-sphere with radius μ is given by

$$x^{(\mu)} x^{(\mu)} + y^{(\mu)} y^{(\mu)} + z^{(\mu)} z^{(\mu)} = \mu^2. \quad (3.25)$$

or

$$x_i^{(\mu)} = \mu x_i. \quad (3.26)$$

Apparently, the μ plays the role of the deformation parameter of the expanding two-sphere. Since the $SO(3)$ global symmetry is preserved in the evolution process, the degeneracy of each Landau level is not lifted. We expect that the matrix geometry obtained will realize an expanding fuzzy two-sphere. Since the number of points of the fuzzy sphere is preserved in this scheme, the only possibility to realize the expanding fuzzy sphere is that the non-commutative length itself grows with the evolution.⁶

We consider the Landau Hamiltonian on the sphere with radius μ :

$$H^{(\mu)} = -\frac{1}{2M\mu^2} \left(\partial_\theta^2 + \cot \theta \partial_\theta + \frac{1}{\sin^2 \theta} (\partial_\phi - iA_\phi)^2 \right) = \frac{1}{\mu^2} H, \quad (3.27)$$

where H is (3.9). The energy eigenstates and the corresponding eigenstates are readily obtained as

$$E_N^{(\mu)} = \frac{1}{\mu^2} E_N, \quad Y_{N,n}^{(\mu)} = \frac{1}{\mu} Y_{N,m}(\theta, \phi), \quad (3.28)$$

where E_N is given by (3.16) and $Y_{N,m}$ are the monopole harmonics. Note that $Y_{N,n}^{(\mu)}$ are normalized on the surface of the two-sphere with radius μ . See Fig.3 for the spectral flow of $E^{(\mu)}$. The degeneracy in each Landau level is not lifted in the process. We can easily derive the matrix coordinates as

$$(X_i^{(\mu)})_{mn} = \int \mu^2 d\theta d\phi \sin \theta Y_{N,m}^{(\mu)}(\theta, \phi)^* x_i^{(\mu)} Y_{N,n}^{(\mu)}(\theta, \phi) = \mu (X_i)_{mn}, \quad (3.29)$$

which satisfy

$$\sum_{i=1}^3 X_i^{(\mu)} X_i^{(\mu)} = \mu^2 \sum_{i=1}^3 X_i X_i, \quad [X_i^{(\mu)}, X_j^{(\mu)}] = i\mu\alpha(I, N) \sum_{k=1}^3 \epsilon_{ijk} X_k^{(\mu)}. \quad (3.30)$$

Here, X_i are given by (3.18). As anticipated, (3.29) shows that the expansion of the fuzzy sphere geometry in accordance with the behavior of the original classical geometry (3.26). The non-commutative parameter becomes $\mu\alpha(I, N)$ as shown in the second equation of (3.30), and it grows as the classical sphere expands. With this is a simple demonstration, we confirmed the plausibility of the present scheme.

⁶The non-unitary evolution of the fuzzy space is discussed by Sasakura [56]. In the paper, the non-commutative scale is fixed and the dimensions of the irreducible representation change in the evolution process, and so the non-unitary evolution takes place.

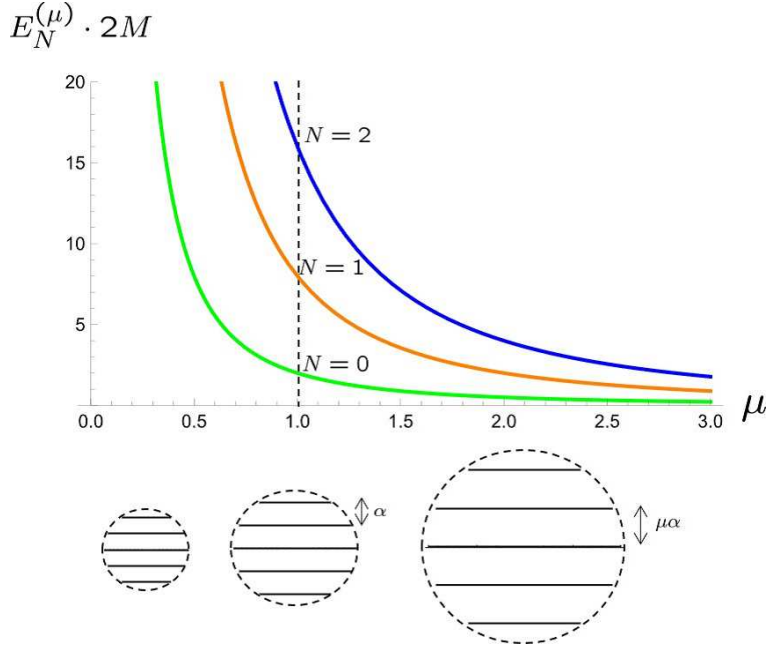


Figure 3: The spectral flow of $E_N^{(\mu)}$ (3.28) for $I/2 = 2$ and $N = 0, 1, 2$ (green, orange, blue). The degeneracy in each Landau level is not lifted.

4 Classical ellipsoidal geometry and magnetic field

Next, we apply this scheme to derive ellipsoidal matrix geometries. The classical evolution process is shown in Fig.4. As the evolution process does not respect the $SU(2)$ symmetry, the degeneracy of each Landau level is lifted. Then, tracing the spectral flow will be crucial to identify the eigenstates needed. As a preparation, this section introduces the basic geometry and algebraic structure of the classical ellipsoid.

4.1 Geometric quantities

We introduce ellipsoid as

$$x^2 + y^2 + \left(\frac{z}{\mu}\right)^2 = 1, \quad (4.1)$$

where $\mu (> 0)$ denotes the deformation parameter of the ellipsoid. We call the limit $\mu \rightarrow 1/0$ the sphere-limit/squashed-sphere-limit in this paper. We parameterize the ellipsoid in the ellipto-spherical coordinates [69]:

$$x = \sin \theta \cos \phi, \quad y = \sin \theta \sin \phi, \quad z = \mu \cos \theta, \quad (4.2)$$

where $\theta = [0, \pi]$ and $\phi = [0, 2\pi)$. The area element of the ellipsoid is given by (A.9)

$$d\Omega = \rho \sin \theta d\theta \wedge d\phi = d\Omega_\phi(\theta) \wedge d\phi, \quad (4.3)$$

where

$$\rho := \sqrt{\mu^2(x^2 + y^2) + \frac{1}{\mu^2}z^2} = \sqrt{\cos^2 \theta + \mu^2 \sin^2 \theta}. \quad (4.4)$$

As in the S^2 case, we will take the symplectic form as the area element (4.3). Then, the symplectic potential Ω is given by

$$\Omega = \left(\int \rho \sin \theta d\theta \right) \wedge d\phi. \quad (4.5)$$

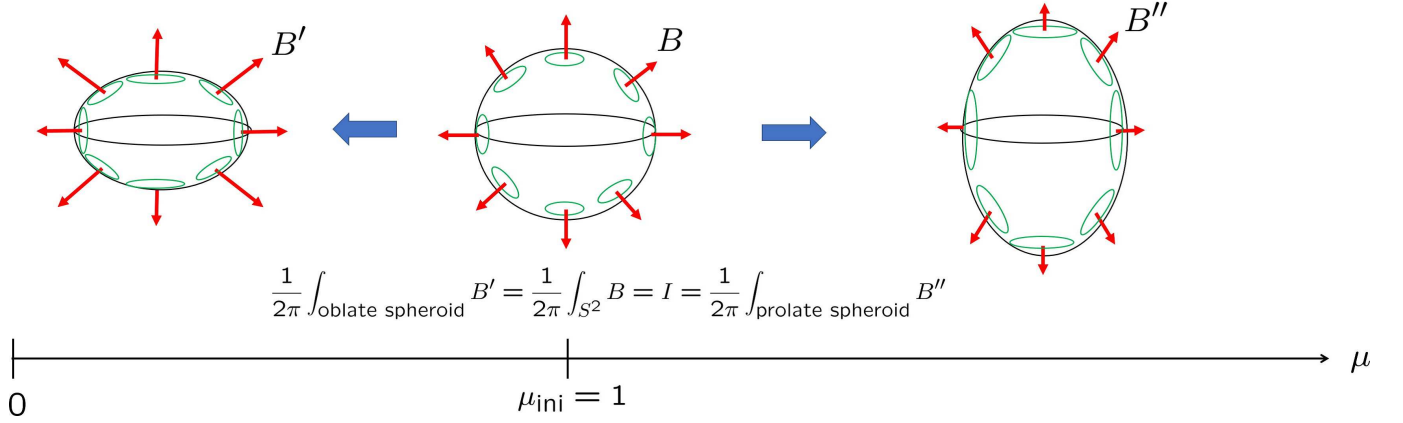


Figure 4: Deformation from sphere to ellipsoids. The $\mu_{\text{ini}} = 1$ is the reference point at which the two-sphere is realized. The $\mu < 1$ represents an oblate spheroid (the limit $\mu \rightarrow 0$ corresponds to the squashed sphere [68]), while the $\mu > 1$ denotes a prolate spheroid.

The integral is evaluated as

$$\int \rho \sin \theta d\theta = \Omega_\phi(\theta) + f(\phi) \quad (4.6)$$

with $f(\phi)$ being an arbitrary function of ϕ and⁷

$$\Omega_\phi(\theta) = -\frac{1}{2}(1 + \rho \cos \theta) - \frac{\mu^2}{\sqrt{\mu^2 - 1}} \text{Arctan} \left(\frac{1 - \rho}{\sqrt{\mu^2 - 1}} \frac{1}{1 + \cos \theta} \right). \quad (4.8)$$

In the limit $\mu \rightarrow 1$, $\Omega_\phi(\theta)$ is reduced to ζ (3.6):

$$\Omega_\phi(\theta) \rightarrow \zeta(\theta) = -\cos \theta, \quad (4.9)$$

which has the mirror symmetry with respect to $z = 0$, *i.e.*, $\zeta(\pi - \theta) = -\zeta(\theta)$. Meanwhile, $\Omega_\phi(\theta)$ itself does not have the mirror symmetry:

$$\Omega_\phi(\theta) \neq -\Omega_\phi(\pi - \theta). \quad (\mu \neq 1) \quad (4.10)$$

Using the degrees of freedom $f(\phi)$, we introduce the following symplectic potential

$$\Omega_\phi(\theta) = \frac{1}{2}(\Omega_\phi(\theta) - \Omega_\phi(\pi - \theta)), \quad (4.11)$$

which has the mirror symmetry,

$$\Omega_\phi(\pi - \theta) = -\Omega_\phi(\theta). \quad (4.12)$$

The explicit form of $\Omega_\phi(\theta)$ is given by⁸

$$\Omega_\phi(\theta) = -\frac{1}{2}\rho \cos \theta - \frac{\mu^2}{2\sqrt{\mu^2 - 1}} \text{Arctan} \left(\frac{1 - \rho}{\sqrt{\mu^2 - 1}} \frac{1}{1 + \cos \theta} \right) + \frac{\mu^2}{2\sqrt{\mu^2 - 1}} \text{Arctan} \left(\frac{1 - \rho}{\sqrt{\mu^2 - 1}} \frac{1}{1 - \cos \theta} \right). \quad (4.15)$$

⁷For $\mu < 1$, we can represent (4.8) as

$$\Omega_\phi(\theta) = -\frac{1}{2}(1 + \rho \cos \theta) + \frac{\mu^2}{\sqrt{1 - \mu^2}} \text{Arctanh} \left(\frac{1 - \rho}{\sqrt{1 - \mu^2}} \frac{1}{1 + \cos \theta} \right). \quad (4.7)$$

⁸In the Cartesian coordinates, (4.15) is given by

$$\Omega = \sum_{i=1}^3 \Omega_i dx_i, \quad (4.13)$$

It is straightforward to check

$$\partial_\theta \Omega_\phi(\theta) = \rho \sin \theta \quad (4.16)$$

and

$$\Omega_\phi(\theta) \xrightarrow{\mu \rightarrow 1} -\cos \theta. \quad (4.17)$$

In the following, we adopt $\Omega_\phi(\theta)d\phi$ (4.15) as our symplectic potential. For the sphere, the spin connection coincides with the symplectic potential, $-\cos \theta d\phi$, while for the ellipsoid they are different (compare (A.6) and (4.17)).

4.2 Classical algebra of ellipsoid-coordinates

While the ellipsoid is obviously symmetric around the $SO(2)$ rotation around the z -axis, it also has a “hidden” $SO(3)$ symmetry: When we rescale z by μz , the ellipsoid is reduced a two-sphere to have the $SO(3)$ rotational symmetry. Indeed, the ellipsoid (4.1) is apparently symmetric for the $SO(2)$ rotation around the z -axis generated by

$$L_z = -ix\partial_y + iy\partial_x = -i\partial_\phi, \quad (4.18)$$

and also symmetric under the rotations generated by the following operators,

$$L_x = -i\mu y\partial_z + i\frac{1}{\mu}z\partial_y = i\sin \phi\partial_\theta + i\cos \phi \cot \theta\partial_\phi, \quad L_y = -i\frac{1}{\mu}z\partial_x + i\mu x\partial_z = -i\cos \phi\partial_\theta + i\sin \phi \cot \theta\partial_\phi. \quad (4.19)$$

They obviously satisfy the $SO(3)$ algebra, $[L_i, L_j] = i\sum_{k=1}^3 \epsilon_{ijk} L_k$. Meanwhile, the classical algebra on ellipsoid only respects the $SO(2)$ symmetry as we shall see below. With the symplectic form (4.5), Ω_ϕ (4.15) and ϕ may signify the Darboux coordinates (canonical coordinates) of the ellipsoid, and the Poisson bracket is represented as

$$\{f, g\} = \frac{\partial f}{\partial \Omega_\phi} \frac{\partial g}{\partial \phi} - \frac{\partial f}{\partial \phi} \frac{\partial g}{\partial \Omega_\phi} = \frac{1}{\sqrt{\cos^2 \theta + \mu^2 \sin^2 \theta} \sin \theta} \left(\frac{\partial f}{\partial \theta} \frac{\partial g}{\partial \phi} - \frac{\partial f}{\partial \phi} \frac{\partial g}{\partial \theta} \right). \quad (4.20)$$

Then, we have

$$\{x, y\} = \frac{1}{\sqrt{\mu^4(x^2 + y^2) + z^2}} z, \quad \{y, z\} = \frac{\mu^2}{\sqrt{\mu^4(x^2 + y^2) + z^2}} x, \quad \{z, x\} = \frac{\mu^2}{\sqrt{\mu^4(x^2 + y^2) + z^2}} y. \quad (4.21)$$

The Poisson bracket relations (4.21) are covariant under the $SO(2)$ rotation around the z -axis, but not under the $SO(3)$ rotations generated by (4.18) and (4.19). While the ellipsoid geometry (4.1) has the $SO(3)$ symmetry, the classical algebra reduces that $SO(3)$ symmetry to the $SO(2)$ rotational symmetry. Since the ellipsoidal matrix geometries obtained are expected to satisfy a quantum version of the classical algebra (4.21), they will have the $U(1)$ symmetry rather than the $SU(2)$ symmetry.

Also notice that (4.21) is expanded by $\delta\mu := \mu - 1$ as

$$\{x, y\} \simeq z - \delta\mu \cdot z(2 - z^2), \quad \{y, z\} \simeq x + \delta\mu \cdot xz^2, \quad \{z, x\} \simeq y + \delta\mu \cdot yz^2, \quad (4.22)$$

where $x^2 + y^2 = 1 - \frac{1}{\mu^2}z^2$ was used. The algebra signifies a highly nonlinear dependence of the coordinates unlike the case of two-sphere ($\delta\mu = 0$).

with

$$\Omega_i = \frac{1}{x^2 + y^2} \sum_{j=1}^3 \epsilon_{ij3} x_j \cdot \left(\frac{\rho}{2\mu} z + \frac{\mu^2}{2\sqrt{\mu^2 - 1}} \text{Arctan} \left(\frac{1 - \rho}{\sqrt{\mu^2 - 1}} \frac{\mu}{\mu + z} \right) - \frac{\mu^2}{2\sqrt{\mu^2 - 1}} \text{Arctan} \left(\frac{1 - \rho}{\sqrt{\mu^2 - 1}} \frac{\mu}{\mu - z} \right) \right). \quad (4.14)$$

In the sphere-limit $\mu \rightarrow 1$, $\Omega_i \rightarrow \frac{z}{\sqrt{x^2 + y^2 + z^2}} \sum_{j=1}^3 \epsilon_{ij3} x_j$, which is the Dirac monopole gauge field in the Schwinger gauge [37].

4.3 Gauge field and magnetic field

We introduce the gauge field to be proportional to the symplectic potential:

$$A = \frac{2\pi I}{S} \Omega_\phi(\theta) d\phi = \frac{2\pi I}{S} \sum_{i=1}^3 \Omega_i dx_i \quad (4.23)$$

where S denotes the area of the ellipsoid (A.10). The present gauge field has the mirror symmetry, and then we refer the present gauge to as the Schwinger gauge. In the sphere-limit, A is reduced to the Dirac monopole gauge field, $A \rightarrow -\frac{I}{2} \cos \theta d\phi$, while in the squashed-sphere limit, $A \rightarrow -\frac{I}{2} \cos^2 \theta d\phi$. The corresponding magnetic field is proportional to the symplectic form:

$$F = dA = \frac{2\pi I}{S} d\Omega = \frac{2\pi I}{S} \rho \sin \theta d\theta \wedge d\phi = F_{\theta\phi} d\theta \wedge d\phi, \quad (4.24)$$

where

$$F_{\theta\phi} = -F_{\phi\theta} = \partial_\theta A_\phi - \partial_\phi A_\theta = \frac{2\pi I}{S} \partial_\theta \Omega_\phi = \frac{2\pi I}{S} \rho \sin \theta. \quad (4.25)$$

Here, I is the first Chern number corresponding to the monopole charge

$$\frac{1}{2\pi} \int_{\text{ellipsoid}} F = I. \quad (4.26)$$

Notice that the field strength (4.25) is invariant under the parallel transport on the ellipsoid,

$$\nabla_\mu F_{\nu\rho} = \partial_\mu F_{\nu\rho} - \Gamma^\lambda_{\mu\nu} F_{\lambda\rho} - \Gamma^\lambda_{\mu\rho} F_{\nu\lambda} = 0. \quad (4.27)$$

This means that the present magnetic field is uniform on the ellipsoid and compatible with the symmetry of the ellipsoid. It is important to take the gauge field configuration to be compatible with the geometry of the manifold, otherwise the matrix geometry obtained will not have the same symmetry as the original classical manifold. Since the gauge field owes its origin to the geometry of the manifold (and indeed the gauge field is essentially the symplectic potential), the gauge field is not a fixed configuration, but it evolves along with the deformation of the ellipsoid.⁹

Let us regard this system as a 2D system embedded in \mathbb{R}^3 . In the whole \mathbb{R}^3 space, there are an infinite number of magnetic fields that yield (4.24) on the ellipsoid. Typical examples of such 3D magnetic fields are

$$B_i := \frac{2\pi I}{Sr^4} \sqrt{x^2 + y^2 + \frac{1}{\mu^4} z^2} x_i, \quad (4.28)$$

and

$$B'_i := \frac{2\pi I}{Sr^2} n_i, \quad (4.29)$$

where

$$r := \sqrt{x^2 + y^2 + \frac{1}{\mu^2} z^2}, \quad (4.30)$$

and n_i denote the normal vector to the surface of the ellipsoid¹⁰

$$(n_x, n_y, n_z) = \frac{1}{\rho} (\mu x, \mu y, \frac{1}{\mu} z). \quad (4.32)$$

⁹In Ref.[65], Matsuura and Tsuchiya analyzed the Berezin-Toeplitz quantization of ellipsoid. Their gauge field configuration is a *fixed* Dirac monopole unlike the present gauge field (4.23). Then, their model is different from the present model.

¹⁰The normal vector (4.32) can be derived by the formula, $\mathbf{n} = \frac{1}{|\frac{\partial \mathbf{x}}{\partial \theta} \times \frac{\partial \mathbf{x}}{\partial \phi}|} \frac{\partial \mathbf{x}}{\partial \theta} \times \frac{\partial \mathbf{x}}{\partial \phi}$. Also from Eq.(4.1), we have

$$x dx + y dy + \frac{1}{\mu^2} z dz = 0, \quad (4.31)$$

and then $(n_x, n_y, n_z) \propto (x, y, \frac{1}{\mu^2} z)$.

The \mathbf{B}' (4.29) is obviously orthogonal to the surface of the ellipsoid. In both cases, they have the same component perpendicular to the ellipsoid:

$$B_{\perp} := \mathbf{B} \cdot \mathbf{n} = \mathbf{B}' \cdot \mathbf{n} = \frac{2\pi I}{S}. \quad (4.33)$$

This is consistent with the uniformity of the magnetic field (4.27). With (4.33), we can simply reproduce (4.26) as

$$\frac{1}{2\pi} \int_{\text{ellipsoid}} B_{\perp} d\Omega = I. \quad (4.34)$$

Since the electron confined to the surface of the ellipsoid only feels the Lorentz force induced by the perpendicular component of the magnetic field, these two magnetic fields affect the electron in the exactly same way. Note, however, from the perspective of the existence of a vector potential in the 3D space, \mathbf{B} is more plausible than \mathbf{B}' . This is because the divergence of \mathbf{B}' does not vanish ($\text{div}\mathbf{B}' \neq 0$), which implies that there is no gauge potential \mathbf{A}' that gives \mathbf{B}' by $\mathbf{B}' = \text{rot}\mathbf{A}'$. Meanwhile, the divergence of \mathbf{B} vanishes (except for the origin), $\text{div}\mathbf{B} = 0$ ($\mathbf{x} \neq 0$), and there exists a gauge potential \mathbf{A} for the \mathbf{B} . Indeed, $\mathbf{A} = \frac{2\pi I}{S}\mathbf{\Omega}$ (4.14) gives \mathbf{B} by $\text{rot}\mathbf{A} = \mathbf{B}$.

The magnetic field \mathbf{B} (4.28) has the singularity at the origin $x = y = z = 0$, and the field configuration is radial but not spherically symmetric. The distribution of the magnetic field (4.28) is axially symmetric around the z -axis just like the ellipsoid. While the ellipsoid is transformed into a sphere by $z \rightarrow \mu z$ as mentioned in Sec.4.2, \mathbf{B} (4.28) is not transformed to the magnetic field of the Dirac monopole by the scale transformation. The existence of the magnetic field reduces the symmetry of the system from $SO(3)$ to $SO(2)$. The magnitude of \mathbf{B} is given by

$$B = \frac{2\pi I}{Sr^4} \sqrt{\left(x^2 + y^2 + \frac{1}{\mu^4}z^2\right)\left(x^2 + y^2 + z^2\right)}. \quad (4.35)$$

On the surface of an ellipsoid ($r = 1$), (4.35) is reduced to

$$B|_{r=1} = \frac{2\pi I}{S} \sqrt{\left(1 - \frac{1}{\mu^4}(\mu^2 - 1)z^2\right)\left(1 + \frac{1}{\mu^2}(\mu^2 - 1)z^2\right)}. \quad (4.36)$$

At the sphere-limit ($\mu \rightarrow 1$), the magnetic field becomes constant $B = \frac{I}{2\pi}$. See Fig.5 for the configurations of \mathbf{A} and \mathbf{B} .

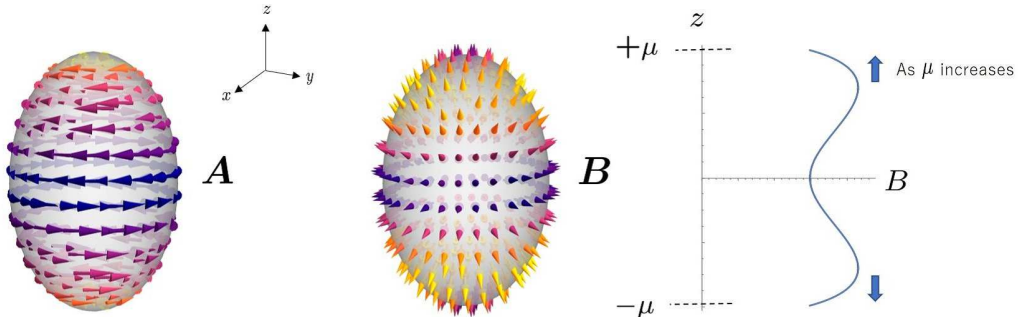


Figure 5: Left: The distribution of the gauge field \mathbf{A} on the ellipsoid (4.23). Middle: The distribution of the magnetic field \mathbf{B} (4.28). Right: The magnitude of the magnetic field exhibits a non-trivial dependence on z (4.35). The two peaks move to the directions of the blue arrows as μ increases.

5 Non-relativistic Landau model and matrix geometries

In this section, we numerically solve the eigenvalue problem of the Landau model on ellipsoid to derive ellipsoidal matrix geometry.

5.1 Symmetry and eigenvalue problem on an ellipsoid

From the general formula of the Laplace-Beltrami operator on the Riemannian manifold

$$\Delta = \frac{1}{\sqrt{g}}(\partial_\mu + iA_\mu)(\sqrt{g}g^{\mu\nu}(\partial_\nu + iA_\nu)), \quad (5.1)$$

we can easily construct the Landau Hamiltonian on the ellipsoid as

$$H^{(\mu)} = -\frac{1}{2M} \left(\frac{1}{\rho^2} \partial_\theta^2 + \cot \theta \frac{1}{\rho^4} \partial_\theta + \frac{1}{\sin^2 \theta} (\partial_\phi + iA_\phi(\theta))^2 \right). \quad (5.2)$$

At $\mu = 1$, (5.2) is reduced to the Landau Hamiltonian on a two-sphere (3.9), which respects the $SU(2)$ rotational symmetry. Recall that ρ and A_ϕ depend on the deformation parameter μ . The Landau Hamiltonian (5.2) is commutative with

$$L_z = -ix \frac{\partial}{\partial y} + iy \frac{\partial}{\partial x} = -i \frac{\partial}{\partial \phi}, \quad (5.3)$$

which means that this Hamiltonian has the $U(1)$ axially symmetry around the z -axis and the L_z is a conserved quantity. Hence, the magnetic quantum number m is a good quantum number during the evolution process.

Since the system is axially symmetric around the z -axis, we may assume that the eigenstates of $H^{(\mu)}$ are expressed as

$$\psi^{(\mu)}(\theta, \phi) = \Theta^{(\mu)}(\theta) e^{im\phi}, \quad (5.4)$$

where m is the magnetic quantum number. The eigenvalue problem on the ellipsoid is reduced to the 1D eigenvalue problem on the latitude with the polar angle θ :

$$-\frac{1}{2M} \left(\frac{1}{\rho^2} \frac{d^2}{d\theta^2} + \cot \theta \frac{1}{\rho^4} \frac{d}{d\theta} - \frac{1}{\sin^2 \theta} (m + A_\phi(\theta))^2 \right) \Theta(\theta) = E \Theta(\theta). \quad (5.5)$$

To solve (5.5) with an analytical method will be a formidable task. We then use the function of the Mathematica, “NDEigensystem”, and numerically derive its eigenvalues and eigenstates. We will consider a deformation from a sphere to an ellipsoid by changing the parameter μ . In addition to the $U(1)$ symmetry, the Hamiltonian possesses the \mathbb{Z}_2 reflection symmetry with respect to the xy -plane ($z = 0$):

$$z \rightarrow -z \quad \text{or} \quad \theta \rightarrow \pi - \theta. \quad (5.6)$$

As a result, the energy eigenvalues for m and $-m$ are always degenerate.

Before proceeding to details, it may be worthwhile to explain how we can solve (5.5) numerically in the case of the sphere ($\mu = 1$).¹¹ The Landau level is indexed by a non-negative integer N , and the range of the magnetic quantum number is given by (3.17). Fig.6 represents the allowed values of m for a given N . Meanwhile, when we numerically solve the Landau problem using (5.5), we first need to specify m as the input parameter of (5.5). By solving (5.5), we later determine the N th energy eigenvalues of the Landau level. From Fig.6, we see that the allowed values of N obviously depend on m as

$$\text{For } |m| \leq \frac{I}{2}, \quad N = 0, 1, 2, 3, \dots, \quad (5.7a)$$

$$\text{For } |m| > \frac{I}{2}, \quad N = |m| - \frac{I}{2}, |m| + 1 - \frac{I}{2}, |m| + 2 - \frac{I}{2}, |m| + 3 - \frac{I}{2}, \dots. \quad (5.7b)$$

¹¹For a sphere, we can solve the Landau problem analytically (see Sec.3).

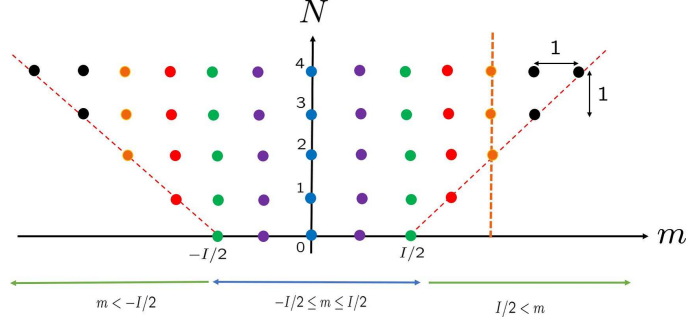


Figure 6: The Landau levels with $I/2 = 2$ for the sphere ($\mu = 1$) and the range of the magnetic quantum number. The vertical dashed orange line represents $m = \frac{I}{2} + 2$, which concerns $N \geq 2$ Landau levels.

Note that if we enter $|m| > I/2$ in (5.5), the lowest energy obtained does *not* start from the lowest Landau level ($N = 0$), but from the $N = (|m| - \frac{I}{2})$ th Landau level. Similar cares have to be taken when solving (5.5) numerically in the case of the ellipsoid: If we want to know the evolution of the N th Landau level, we must first enter an m ($|m| \leq N + \frac{I}{2}$) in Eq.(5.5) and solve the eigenvalue equation numerically. Then we choose the N th energy eigenvalue from the lowest for $|m| \leq I/2$, while $N - |m| + I/2$ th for $|m| > I/2$. That eigenvalue realizes the evolved energy of the eigenstate with quantum magnetic number m of the N th Landau level. We repeat this procedure for all m s in the region, $-N - \frac{I}{2} \leq m \leq N + \frac{I}{2}$.

5.2 Evolution of the Landau levels and matrix geometries

We now solve the eigenvalue problem of the Landau Hamiltonian (5.2)

$$H^{(\mu)}\psi_{N,m}^{(\mu)}(\theta, \phi) = E_{N,m}^{(\mu)}\psi_{N,m}^{(\mu)}(\theta, \phi), \quad (5.8)$$

where $\psi_{N,m}^{(\mu)}(\theta, \phi)$ are normalized on the ellipsoid:

$$\langle \psi_{N,m}^{(\mu)} | \psi_{N',m'}^{(\mu)} \rangle = \int_{\text{ellipsoid}} d\Omega \psi_{N,m}^{(\mu)}(\theta, \phi)^* \psi_{N',m'}^{(\mu)}(\theta, \phi) = \delta_{N,N'} \delta_{m,m'}. \quad (5.9)$$

Here, $d\Omega$ is given by the are element of the ellipsoid (4.3) and at the sphere-limit ($\mu = 1$) the eigenstates are reduced to the monopole harmonics, $\psi_{N,m}^{(\mu=1)}(\theta, \phi) = Y_{N,m}(\theta, \phi)$. Fig.7 represents the spectral flow of $E_{N,m}^{(\mu)}$. One may see that the N (≥ 1)th Landau level is split into $N + [I/2] + 1$ energy levels¹² as μ changes from $\mu = 1$. Fig.7 also shows that for the oblate spheroid ($\mu < 1$) the energy levels are in the inverse order of $|m|$, while for the prolate spheroid ($\mu > 1$) the energy levels are in the order of $|m|$. The eigenstates are also derived numerically. From Fig.7, we find that the degeneracy of the lowest Landau level is not lifted, but the lowest Landau level eigenstates evolve in the degenerate level during the deformation. The absolute values of the evolving lowest Landau level eigenstates are depicted in Fig.8. One may find that the the set of the eigenvalues is generally elongated along the z axis as μ increases. This behavior qualitatively follows that of the classical ellipsoid.

As discussed in Sec.3, *each* Landau level develops its matrix geometry. We apply the level projection to the $N + [I/2] + 1$ energy levels that originate from the N th Landau level:

$$(X_i^{(\mu)})_{mn} = \langle \psi_{N,m}^{(\mu)} | x_i | \psi_{N,n}^{(\mu)} \rangle = \int_{\text{ellipsoid}} d\Omega \psi_{N,m}^{(\mu)}(\theta, \phi)^* x_i \psi_{N,n}^{(\mu)}(\theta, \phi) \quad (5.10)$$

¹²for even I , each of the $N + [I/2]$ energy levels is doubly degenerate by the contribution of $\pm m$ and the energy level with $m = 0$ is non-degenerate. For even I , each of the $N + [I/2] + 1$ energy levels is doubly degenerate by the contribution of $\pm m$.

Non-relativistic case $I/2 = 2$

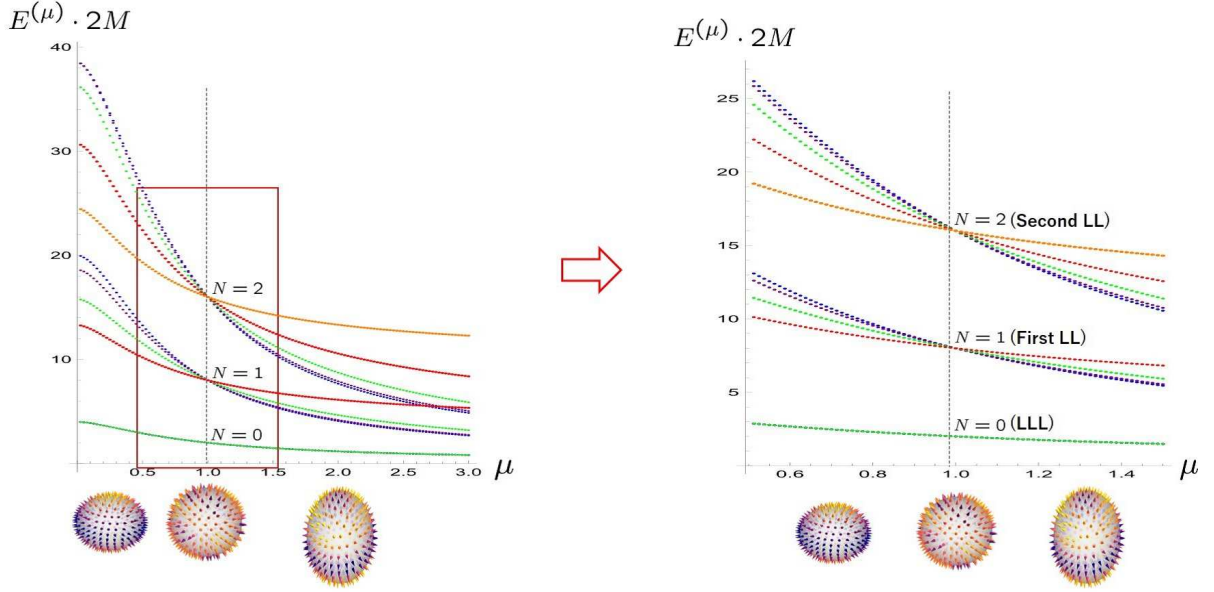


Figure 7: The spectral flow of the non-relativistic Landau model for $I/2 = 2$. In the N th Landau level, there are $2N + 5$ degenerate eigenstates ($-N - 2 \leq m \leq N + 2$). The blue, purple, green, red and orange curves correspond to $m = 0, \pm 1, \pm 2, \pm 3$ and ± 4 , respectively (each of the curves is doubly degenerate except for the blue curve $m = 0$). This coloring corresponds to that of Fig.6. At $\mu = 1$, the energy levels converge to the Landau levels and the level crossings occur. Interestingly, the degeneracy of the lowest Landau level is not lifted for arbitrary μ .

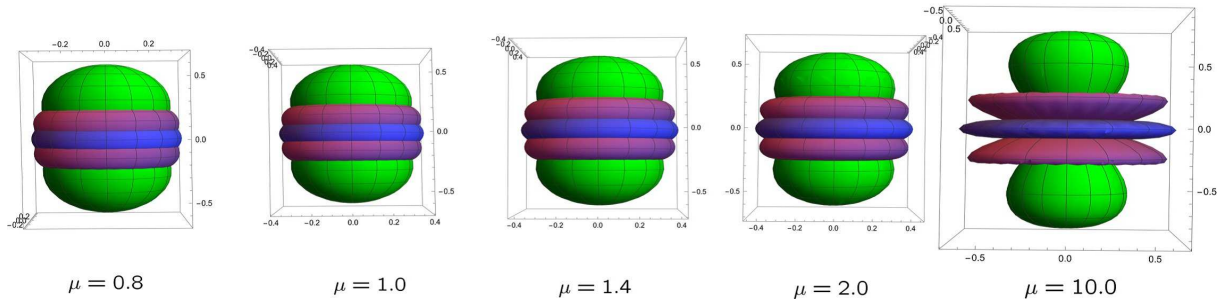


Figure 8: The absolute values of the lowest Landau level eigenstates $\psi_{N=0,m}^{(\mu)}$ of $I/2 = 2$.

or

$$X_i^{(\mu)} = \int_{\text{ellipsoid}} d\Omega x_i (\psi_N^{(\mu)} \psi_N^{(\mu)\dagger})^t. \quad (5.11)$$

The matrix $X_3^{(\mu)}$ realizes the $U(1)$ generator of the rotation around the z -axis. Since the Landau Hamiltonian (5.2) respects only the $U(1)$ rotation symmetry, not the $SU(2)$ symmetry, the obtained matrix ellipsoids are expected to respect the $U(1)$ symmetry only:

$$[X^{(\mu)^2} + Y^{(\mu)^2} + \frac{1}{\mu^2} Z^{(\mu)^2}, Z^{(\mu)}] = 0. \quad (5.12)$$

or

$$[X^{(\mu)^2} + Y^{(\mu)^2}, Z^{(\mu)}] = 0. \quad (5.13)$$

Recall that the $U(1)$ symmetry of the matrix geometry is expected from the discussion in Sec.4.2. We can also show (5.13) with the following general argument. Using the numerically derived matrix coordinates, we can explicitly show that the matrix geometries have the $U(1)$ symmetry (5.13) but not the $SU(2)$ symmetry:

$$[X^{(\mu)^2} + Y^{(\mu)^2} + \frac{1}{\mu^2} Z^{(\mu)^2}, X^{(\mu)}] \neq 0, \quad [X^{(\mu)^2} + Y^{(\mu)^2} + \frac{1}{\mu^2} Z^{(\mu)^2}, Y^{(\mu)}] \neq 0. \quad (5.14)$$

Equation (5.13) implies that $X^{(\mu)^2} + Y^{(\mu)^2}$ and $Z^{(\mu)}$ can be diagonalized simultaneously. Since $x \pm iy$ and z carry the quantum magnetic number $m = \pm 1$ and 0 respectively, the selection rule tells

$$(X^{(\mu)} + iY^{(\mu)})_{mn} := \langle \psi_{N,m}^{(\mu)} | (x + iy) | \psi_{N,n}^{(\mu)} \rangle = g_m^{(\mu)} \delta_{m,n+1}, \quad (5.15a)$$

$$(X^{(\mu)} - iY^{(\mu)})_{mn} := \langle \psi_{N,m}^{(\mu)} | (x - iy) | \psi_{N,n}^{(\mu)} \rangle = g_n^{(\mu)*} \delta_{m+1,n}, \quad (5.15b)$$

$$(Z^{(\mu)})_{\alpha\beta} := \langle \psi_{N,m}^{(\mu)} | z | \psi_{N,n}^{(\mu)} \rangle = f_m^{(\mu)} \delta_{mn}, \quad (5.15c)$$

with $f_m^{(\mu)} \in \mathbb{R}$. The mirror symmetry about the xy plane implies that $|g_{-m}^{(\mu)}| = |g_{m+1}^{(\mu)}|$ and $f_{-m}^{(\mu)} = -f_m^{(\mu)}$. Then, we have

$$\begin{aligned} (X^{(\mu)^2} + Y^{(\mu)^2})_{mn} &= \frac{1}{2} ((X^{(\mu)} + iY^{(\mu)})(X^{(\mu)} - iY^{(\mu)}) + (X^{(\mu)} - iY^{(\mu)})(X^{(\mu)} + iY^{(\mu)}))_{mn} \\ &= \frac{1}{2} (|g_m^{(\mu)}|^2 + |g_{m+1}^{(\mu)}|^2) \delta_{mn} = (X^{(\mu)^2} + Y^{(\mu)^2})_{-m,-n}. \end{aligned} \quad (5.16)$$

Both $X^{(\mu)^2} + Y^{(\mu)^2}$ and $Z^{(\mu)}$ are diagonal matrices, and so they are obviously commutative (5.13).

As $Z^{(\mu)}$ is a diagonal matrix, its diagonal matrix components $f_m^{(\mu)}$ do not depend on the phases of the basis states. Meanwhile, $X^{(\mu)}$ and $Y^{(\mu)}$ have off diagonal components g_m that depend on the relative phases of the basis states. However as indicated by (5.16), the sum of their squares is determined only by the absolute values of g s. Therefore, the matrix counterpart of (4.1)

$$X^{(\mu)^2} + Y^{(\mu)^2} + \frac{1}{\mu^2} Z^{(\mu)^2} \quad (5.17)$$

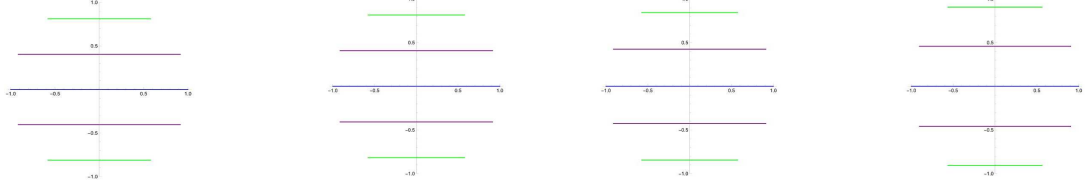
is not relevant to the phases of the basis states.

Figure 9 exhibits the numerically obtained ellipsoidal matrix geometries for $N = 0$ and $N = 1$. To reduce the overall scaling, we used the normalized matrix coordinates:

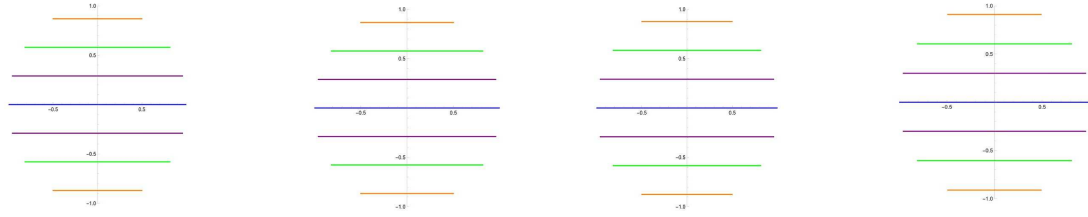
$$\hat{X}_i^{(\mu)} := \frac{1}{\max(\sqrt{X^{(\mu)^2} + Y^{(\mu)^2})} } X_i^{(\mu)}, \quad (5.18)$$

so that $\max((\hat{X}^{(\mu)})^2 + (\hat{Y}^{(\mu)})^2) = 1$. It can be seen that the behaviors of the ellipsoidal matrix geometries are quantitatively different in each Landau level, but qualitatively similar: The matrix geometries are generally elongated along the z axis analogous to the eigenstates (Fig.8), as μ increases. (For $\mu < 1$, this tendency is not clear.)

$N = 0$ matrix geometry ($I = 4$)



$N = 0$ matrix geometry ($I = 6$)



$N = 1$ matrix geometry ($I = 4$)

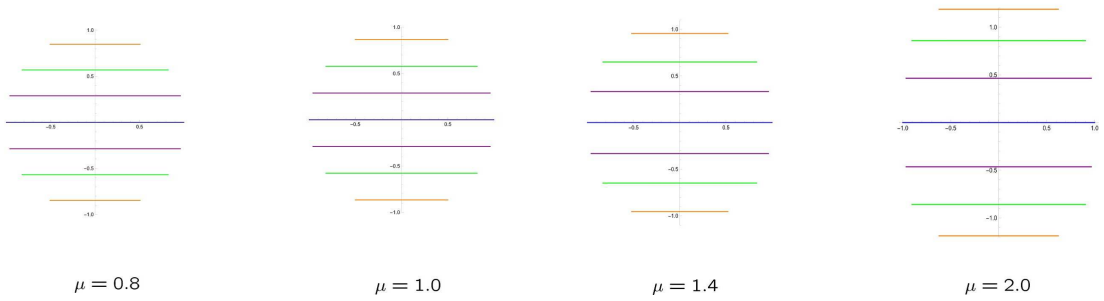


Figure 9: Ellipsoidal matrix geometries in the Landau levels. At $\mu = 1$, the fuzzy sphere geometry is reproduced. The horizontal lengths of the latitudes of the ellipsoidal matrix geometries represent the eigenvalues of $2\sqrt{(\hat{X}_1^{(\mu)})^2 + (\hat{X}_2^{(\mu)})^2}$. The second and third rows denote the evolution of the the matrix geometries with 7×7 matrix size of the lowest and first excited Landau levels, respectively: One may find that the behavior of the ellipsoidal matrix geometry of the lowest Landau level geometry differs from those of the first Landau level.

6 Relativistic Landau models on the ellipsoid

In this section, we generalize the previous non-relativistic analysis to the relativistic case. We consider a relativistic particle on an ellipsoid under the magnetic field.

6.1 Dirac-Landau operator

We introduce gamma matrices, zweibein and the spin-connection as (see Appendix A for details)

$$\begin{aligned} \gamma^{m=1,2} &= \{\sigma_1, \sigma_2\}, \quad e_1^\theta = \frac{1}{\rho}, \quad e_2^\phi = \frac{1}{\sin\theta}, \quad \text{other } e_m^\mu \text{ are zeros,} \\ \omega_\theta &= 0, \quad \omega_\phi(\theta) = \omega_{\phi 12}(\theta)\sigma_{12} = -\frac{1}{2\rho} \cos\theta\sigma_3. \end{aligned} \quad (6.1)$$

With these, we construct the Dirac-Landau operator on the ellipsoid:

$$-i\mathcal{D} = -i \sum_{m=1,2} \sum_{\mu=\theta,\phi} e_m^\mu \gamma^m \mathcal{D}_\mu. \quad (6.2)$$

Here, the covariant derivatives contain both the spin-connection and the gauge connection,

$$\mathcal{D}_\mu := \frac{\partial}{\partial x^\mu} + i(\omega_\mu \otimes 1 - \mathbf{1}_2 \otimes A_\mu), \quad (6.3)$$

where the gauge field is the same as (4.23)

$$A_\theta = 0, \quad A_\phi = \frac{2\pi I}{S} \Omega_\phi(\theta), \quad (6.4)$$

and the corresponding field strength is (4.25). The covariant derivatives (6.2) are expressed as

$$\mathcal{D}_\theta = \partial_\theta, \quad \mathcal{D}_\phi = \partial_\phi + i\omega_\phi - iA_\phi = \partial_\phi - i\frac{1}{2} \frac{\cos\theta}{\rho} \sigma_3 - i\frac{2\pi I}{S} \Omega_\phi, \quad (6.5)$$

and then

$$-i\mathcal{D} = -ie_1^\theta \sigma_1 \frac{\partial}{\partial \theta} - ie_2^\phi \sigma_2 \left(\frac{\partial}{\partial \phi} + i(\omega_\phi - A_\phi) \right). \quad (6.6)$$

The Dirac-Landau operator respects the chiral symmetry for arbitrary values of μ ,

$$\{\sigma_3, -i\mathcal{D}\} = 0. \quad (6.7)$$

Hence, the spectra of the Dirac-Landau operator are symmetric with respect to the zero energy. The Dirac-Landau operator is commutative with $L_z = -i\frac{\partial}{\partial \phi}$:

$$[L_z, -i\mathcal{D}] = 0, \quad (6.8)$$

which implies that the present system is axially symmetric around the z -axis, and the magnetic quantum number can be used as a good quantum number same as in the non-relativistic case. In the matrix representation, the Dirac-Landau operator (6.6) is expressed as

$$-i\mathcal{D} = -i\frac{1}{\rho} \sigma_1 \left(\frac{\partial}{\partial \theta} + \frac{1}{2} \cot\theta \right) - i\frac{1}{\sin\theta} \sigma_2 \left(\frac{\partial}{\partial \phi} - i\frac{2\pi I}{S} \Omega_\phi \right) = -i \begin{pmatrix} 0 & \check{\partial}_- \\ \check{\partial}_+ & 0 \end{pmatrix}, \quad (6.9)$$

where

$$\check{\partial}_\pm := \frac{1}{\rho} \frac{\partial}{\partial \theta} + \frac{1}{2\rho} \cot\theta \pm i\frac{1}{\sin\theta} \left(\frac{\partial}{\partial \phi} - i\frac{2\pi I}{S} \Omega_\phi \right). \quad (6.10)$$

At the reference point ($\mu = 1$), (6.9) is reduced to

$$-i\mathcal{D}|_{\mu=1} = -i \begin{pmatrix} 0 & \frac{\partial}{\partial\theta} - i\frac{1}{\sin\theta}\frac{\partial}{\partial\phi} + (\frac{I}{2} + \frac{1}{2})\cot\theta \\ \frac{\partial}{\partial\theta} + i\frac{1}{\sin\theta}\frac{\partial}{\partial\phi} - (\frac{I}{2} - \frac{1}{2})\cot\theta & 0 \end{pmatrix}, \quad (6.11)$$

which respects the $SU(2)$ rotational symmetry [37]. The eigenvalues are given by

$$-i\mathcal{D}|_{\mu=1} = \pm\sqrt{N(N+I)} \quad (N = 0, 1, 2, 3, \dots) \quad (6.12)$$

with $I + 2N$ degeneracy coming from the $SU(2)$ rotational symmetry:

$$m = N + \frac{I}{2} - \frac{1}{2}, N + \frac{I}{2} - \frac{3}{2}, \dots, -(N + \frac{I}{2} - \frac{1}{2}). \quad (6.13)$$

The difference to the non-relativistic case (3.17) is the $1/2$ reduction of the $SU(2)$ angular momentum index. For arbitrary μ , the Dirac-Landau operator has only the axial symmetry around the z -axis, and then the $SU(2)$ degeneracy of the relativistic Landau level (6.12) is lifted (Fig.10).

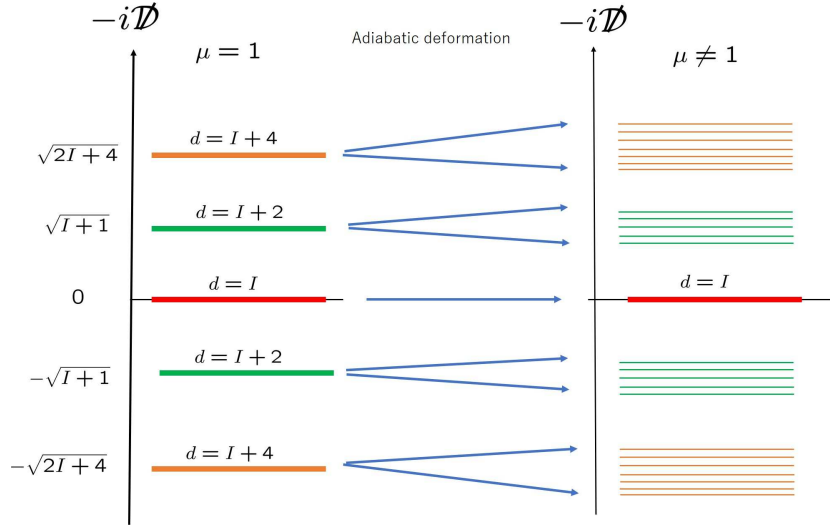


Figure 10: The evolution of the spectra of the Dirac-Landau operator. The spectra of the Dirac-Landau operator are symmetric with respect to the zeroth Landau level. For $\mu = 1$, the relativistic Landau level has the degeneracy due to the $SU(2)$ rotational symmetry. The degeneracy of the zeroth Landau level is not lifted under the deformation as guaranteed by the Atiyah-Singer index theorem (see Sec.6.3).

6.2 Supersymmetric Landau model

The Dirac-Landau operator is a matrix differential operator of off-diagonal blocks (6.9). A standard strategy for deriving the spectra of the Dirac-Landau operator is to take the square of the Dirac-Landau operator and transform it into a diagonal matrix with differential operators. We diagonalize the operators in the diagonal components and take the two square roots of their eigenvalues to realize the spectra of the original Dirac-Landau operator.

From a generalized Lichnerowicz formula [70], the square of the Dirac-Landau operator is given by

$$(-i\mathcal{D})^2 = -\Delta - e_m^\mu e_n^\nu \sigma_{mn} \otimes F_{\mu\nu} + \frac{\mathcal{R}}{4}. \quad (6.14)$$

In the present case, we have

$$(-i\mathcal{P})^2 = -\Delta - e_1^\theta e_2^\phi \sigma_3 F_{\theta\phi} + \frac{\mathcal{R}}{4} = -\Delta - \frac{1}{\rho \sin\theta} \sigma_3 F_{\theta\phi} + \frac{\mathcal{R}}{4}, \quad (6.15)$$

where $\mathcal{R} := 2\frac{\mu^2}{\rho^4}$ represents the scalar curvature, and

$$\Delta := \frac{1}{\sqrt{g}} \mathcal{D}_\mu (\sqrt{g} g^{\mu\nu} \mathcal{D}_\nu) = \frac{1}{\rho^2} \partial_\theta^2 + \cot\theta \frac{1}{\rho^4} \partial_\theta + \frac{1}{\sin^2\theta} \left(\partial_\phi - i \frac{1}{2} \frac{\cos\theta}{\rho} \sigma_3 - i \frac{2\pi I}{S} \Omega_\phi \right)^2. \quad (6.16)$$

With (4.25), (6.15) is expressed as¹³

$$H_{\text{susy}} := (-i\mathcal{P})^2 = -\Delta + \frac{1}{2} \frac{\mu^2}{\rho^4} - \frac{2\pi I}{S} \sigma_3 = \begin{pmatrix} H_+ & 0 \\ 0 & H_- \end{pmatrix}, \quad (6.17)$$

where

$$H_\pm := -\bar{\partial}_\mp \partial_\pm = -\frac{1}{\rho^2} \partial_\theta^2 - \cot\theta \frac{1}{\rho^4} \partial_\theta - \frac{1}{\sin^2\theta} \left(\partial_\phi \mp i \frac{1}{2} \frac{\cos\theta}{\rho} - i \frac{2\pi I}{S} \Omega_\phi \right)^2 + \frac{1}{2} \frac{\mu^2}{\rho^4} \mp \frac{2\pi I}{S}. \quad (6.18)$$

Here, $\bar{\partial}_\pm$ are given by (6.10). Now, we analyze the differential operators in the diagonal components of (6.17). The Hamiltonians, H_+ and H_- , are exchanged under $\phi \rightarrow -\phi$ and $I \rightarrow -I$, and they exhibit the same energy spectra except for the zero energy: For $I > 0$ ($I < 0$), H_+ (H_-) accommodates the zero-modes. The supersymmetric property of the system will become manifest when we rewrite (6.17) as

$$H_{\text{susy}} = \{Q, \bar{Q}\}, \quad (6.19)$$

with supercharges, Q and \bar{Q} ,

$$Q = \mathcal{D}_+ := \frac{1}{2}(1 + \sigma_3)\mathcal{D} = \begin{pmatrix} 0 & \bar{\partial}_- \\ 0 & 0 \end{pmatrix}, \quad \bar{Q} = -\mathcal{D}_- := -\frac{1}{2}(1 - \sigma_3)\mathcal{D} = -\begin{pmatrix} 0 & 0 \\ \bar{\partial}_+ & 0 \end{pmatrix}, \quad (6.20)$$

which are obviously nilpotent operators, $Q^2 = \bar{Q}^2 = 0$. It is easy to see that (6.17) is invariant under the supersymmetric transformations, $[Q, H_{\text{susy}}] = [\bar{Q}, H_{\text{susy}}] = 0$, and then the H_{susy} represents a supersymmetric quantum mechanics on ellipsoid. The supersymmetric Hamiltonian is commutative with the chirality matrix, $[H_{\text{susy}}, \sigma_3] = 0$, while the supercharges are anti-commutative with the chirality matrix, $\{Q, \sigma_3\} = \{\bar{Q}, \sigma_3\} = 0$. Therefore, there are degenerate energy eigenstates of H_{susy} with distinct chirality, which are exchanged by the supersymmetric transformations:

$$|E, \sigma_3 = +1\rangle \xrightarrow{\bar{Q}} |E, \sigma_3 = -1\rangle \xrightarrow{Q} |E, \sigma_3 = +1\rangle \quad (E \neq 0). \quad (6.21)$$

The degenerate eigenstates with distinct chiralities realize the supersymmetric partners. The supersymmetric transformation vanishes the zero-modes:

$$Q|E = 0, \sigma_3\rangle = \bar{Q}|E = 0, \sigma_3\rangle = 0, \quad (6.22)$$

which indicates the zero-modes are supersymmetric invariant states. The zero-modes can be taken as the eigenstates of σ_3 and satisfy

$$-i\mathcal{P} \begin{pmatrix} \psi_m \\ 0 \end{pmatrix} = 0 \quad \rightarrow \quad (-i\mathcal{P})^2 \begin{pmatrix} \psi_m \\ 0 \end{pmatrix} = H_{\text{susy}} \begin{pmatrix} \psi_m \\ 0 \end{pmatrix} = 0. \quad (6.23)$$

¹³One can also explicitly derive (6.17) using (6.9).

The degenerate eigenstates of the zeroth Landau level of the supersymmetric Landau Hamiltonian are equal to the zero-modes of the Dirac-Landau operator. Notice that the above discussion holds for arbitrary μ and that supersymmetry is preserved for any deformation of the ellipsoid.

At the reference point $\mu = 1$, H_{susy} (6.17) is reduced to the supersymmetric Landau Hamiltonian on a sphere [37]:

$$H_{\text{susy}}|_{\mu=1} = -\partial_\theta^2 - \cot \theta \partial_\theta - \frac{1}{\sin^2 \theta} \left(\partial_\phi + i \frac{1}{2} (I-1) \cos \theta \right)^2 + \frac{1}{2} - \frac{I}{2} \sigma_3, \quad (6.24)$$

with eigenvalues

$$N(N+I) \quad (N = 0, 1, 2, 3, \dots) \quad (6.25)$$

and degeneracies

$$d_{N=0} = I + 2N, \quad d_{N=1,2,3,\dots} = 2(I + 2N). \quad (6.26)$$

Relativistic case $I/2 = 5/2$

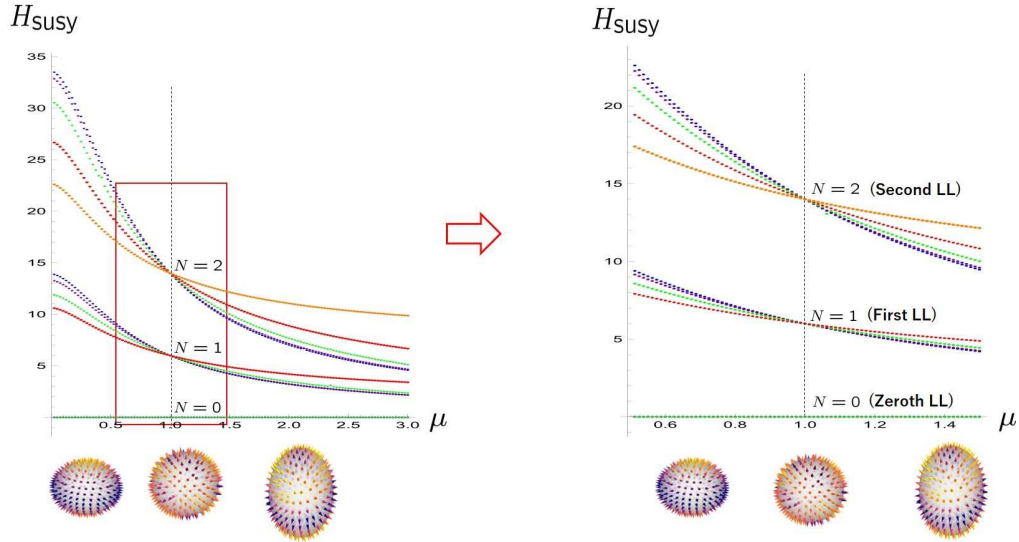


Figure 11: The spectral flow of the supersymmetric Landau model (6.17) for $I/2 = 5/2$. Every spectrum monotonically decreases as μ increases. Note that the degeneracy of the zeroth Landau level is not lifted for any μ . The $N(\geq 1)$ th Landau level accommodates $2 \times (2N + I) = 4N + 10$ degeneracy. (Here, $2 \times$ comes from the spinor degrees of freedom.) The zeroth Landau level accommodates $I = 5$ degeneracy. The blue, purple, green, red and orange curves correspond to $m = 0, \pm 1, \pm 2, \pm 3$ and ± 4 , respectively. Due to the mirror symmetry about the xy -plane, the m and $-m$ eigenstates are always degenerate.

6.3 Zero-modes and the Atiyah-Singer index theorem

We discuss the zero-modes of the Dirac-Landau operator on an ellipsoid and their relation to the Atiyah-Singer index theorem. Let us begin with the reference point $\mu = 1$, at which the spherical relativistic Landau model on two-sphere is realized. The zero-modes can be taken as the eigenstates of σ_3 and satisfy

$$-i\mathcal{D} \begin{pmatrix} \psi_m \\ 0 \end{pmatrix} = 0 \quad \rightarrow \quad -i\mathcal{D}_- \begin{pmatrix} \psi_m \\ 0 \end{pmatrix} = 0, \quad (6.27)$$

where the zero-modes ψ_m ($m = \overbrace{-\frac{I-1}{2}, -\frac{I-1}{2}+1, \dots, \frac{I-1}{2}}^I$) ($N = 0$ in (6.13)) are given by the monopole harmonics at $\mu = 1$ [37]. The index of the Dirac-Landau operator on S^2 is then obtained as

$$\text{Ind}(-i\mathcal{D}) := \dim \text{Ker}(-i\mathcal{D}_-) - \dim \text{Ker}(-i\mathcal{D}_+) = I - 0 = I. \quad (6.28)$$

Meanwhile, the number of the magnetic fluxes is given by

$$\frac{1}{2\pi} \int_{S^2} F = I, \quad (6.29)$$

where $F = \frac{1}{2} \sin \theta d\theta \wedge d\phi$. This exemplifies the Atiyah-Singer index theorem on S^2 :

$$\text{Ind}(-i\mathcal{D})|_{S^2} = \frac{1}{2\pi} \int_{S^2} F. \quad (6.30)$$

The index theorem should hold under a continuous deformation of manifold. We will see this in the following. The right-hand side of (6.30) denotes the number of the fluxes penetrating the surface enclosing the monopole, which is invariant under the continuous deformation of the surface due to Gauss's theorem.¹⁴ Then, we have

$$\frac{1}{2\pi} \int_{S^2} F = \frac{1}{2\pi} \int_{\text{ellipsoid}} F. \quad (6.31)$$

Meanwhile, it is not so obvious that the index of the Dirac-Landau operator is invariant under the continuous deformation, because the energy levels generally evolve, and the degeneracies are usually lifted under the deformation. For the zeroth Landau level, however, this is not the case: Fig.11 clearly shows that the zeroth Landau level remains at the zero energy and the degeneracy is not lifted during the deformation. Therefore, the Dirac-Landau operator on the ellipsoid always accommodates the same number of zero-modes as on the two-sphere:

$$\text{Ind}(-i\mathcal{D})|_{\text{ellipsoid}} = \text{Ind}(-i\mathcal{D})|_{S^2} = I. \quad (6.32)$$

Consequently we confirmed

$$\text{Ind}(-i\mathcal{D})|_{\text{ellipsoid}} = I = \frac{1}{2\pi} \int_{\text{ellipsoid}} F, \quad (6.33)$$

which demonstrates the Atiyah-Singer index theorem on ellipsoid.

7 Ellipsoidal matrix geometry and fuzzy ellipsoid

We investigate basic properties of the ellipsoidal matrix geometries.

7.1 Ellipsoidal matrix geometries

We discuss the ellipsoidal matrix geometry of the the relativistic Landau model. We depict the behavior of the zero-modes in Fig.12. The distribution of the eigenstates is generally elongated along the z direction as the deformation parameter increases. Fig.13 and Fig.14 show the matrix ellipsoids obtained by the zeroth and the first Landau levels of the supersymmetric Landau model. The energy levels of the H_+ and H_- of the supersymmetric Landau Hamiltonian are identical (except for the zero-energy), but the corresponding matrix geometries are different as shown in Fig.14.

¹⁴To be precise, our monopole also evolves in the deformation process, but still (6.31) holds. See (4.26).

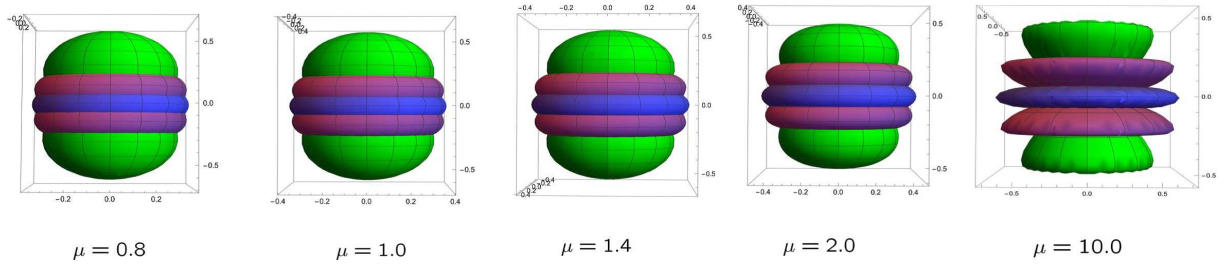


Figure 12: Absolute values of the zero-modes of $I/2 = 5/2$.

Ellipsoidal matrix geometry from zero-modes ($N = 0$)

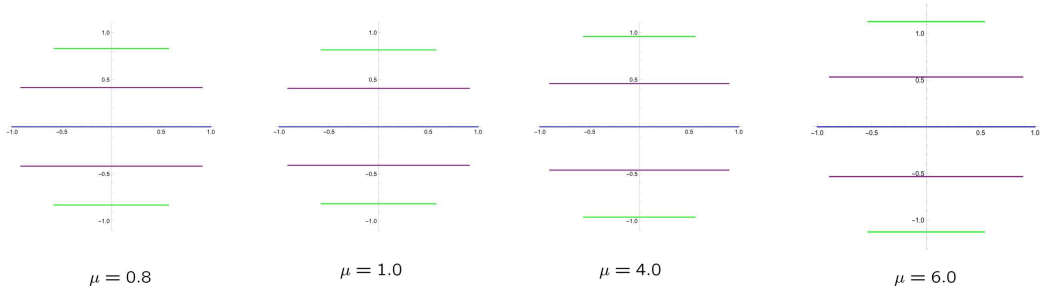


Figure 13: Evolution of the ellipsoidal matrix geometry in the zeroth Landau level of $I/2 = 5/2$. At $\mu = 1$, the fuzzy sphere geometry is realized. The ellipsoidal matrix geometry shows qualitatively similar behavior to the deformation of the original classical ellipsoid.

Ellipsoidal matrix geometry from the relativistic 1st LL ($N = 1$)

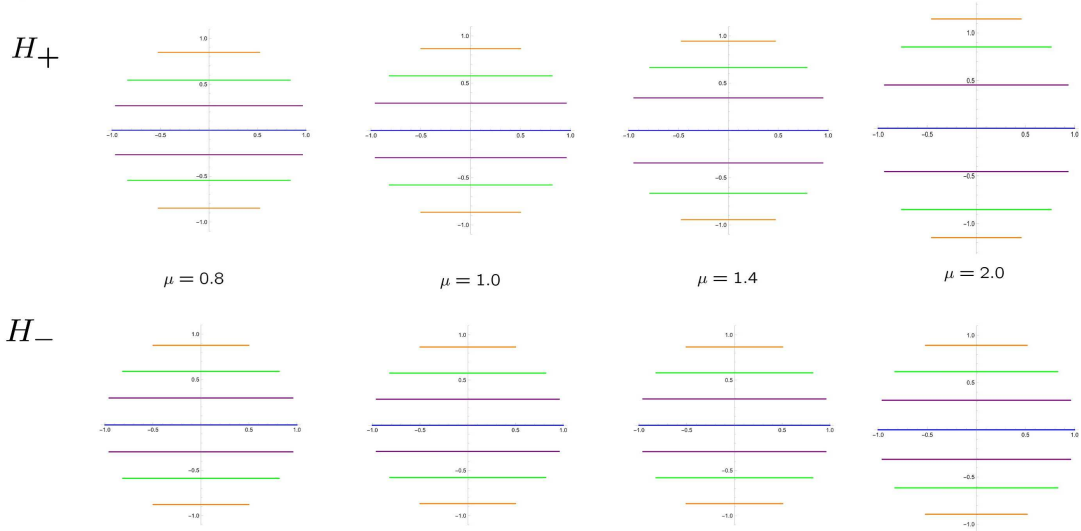


Figure 14: Evolution of the ellipsoidal matrix geometries in the supersymmetric $N = 1$ Landau level of $I/2 = 5/2$. The upper/lower ellipsoidal matrices are derived from the $N = 1$ Landau level eigenstates of $H_{+/-}$.

In the following, we discuss the commutative limit of the ellipsoidal matrix geometry obtained from the zero-modes. We define

$$r(I-1) := \frac{1}{I} \text{tr} \left(\sqrt{X^2 + Y^2 + \frac{1}{\mu^2} Z^2} \right). \quad (7.1)$$

At $\mu = 1$, $r(I-1)$ is reduced to the radius of the fuzzy sphere (3.24) $r(I-1)|_{\mu=1} = \sqrt{\frac{I-1}{I+1}}$. The behavior of (7.1) is depicted in the left of Fig.15. In the continuum limit ($I \rightarrow \infty$), the classical ellipsoid is expected to be realized, *i.e.*, $\lim_{I \rightarrow \infty} r(I-1) = 1$. The left of Fig.15 is consistent with this expectation. We next

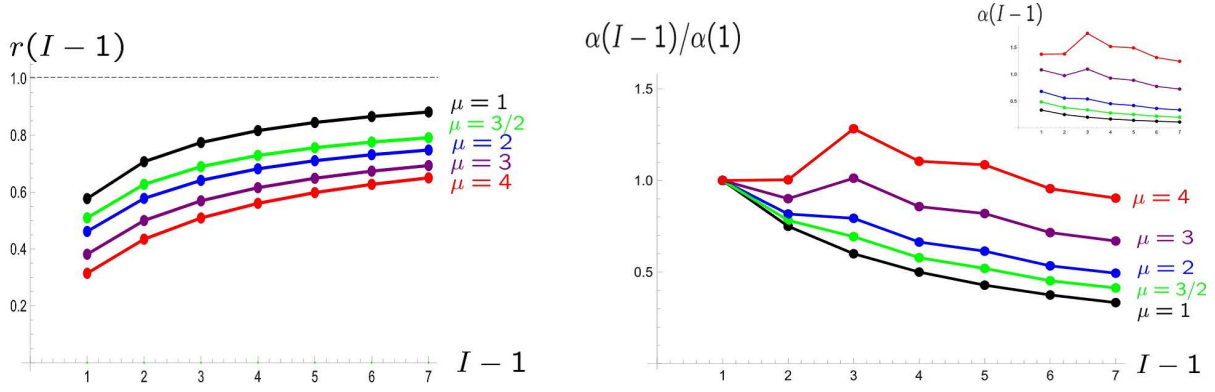


Figure 15: Left: the behaviors of (7.1). Right: The ratio $\alpha(I-1)/\alpha(1)$ (7.3).

examine the behavior of the non-commutative scale in the commutative limit $I \rightarrow \infty$. In the commutative limit, the non-commutative scale should converge to zero. Considering the the first equation of (4.21), we introduce the non-commutative scale as¹⁵

$$\alpha(I-1) := \sum_{m>0}^{(I-1)/2} \frac{([X, Y])_{mm}}{\left(i \frac{1}{\sqrt{\mu^4(x^2+y^2)+z^2}} z \right)_{mm}}. \quad (7.3)$$

At sphere limit $\mu \rightarrow 1$, (7.3) is reduced to the non-commutative scale of the fuzzy sphere (3.23). Fig.15 show that the ratios $\alpha(I-1)/\alpha(1)$ for different μ s. The ratios $\alpha(I-1)/\alpha(1)$ decrease with increasing I . This implies that the ellipsoidal matrix geometries approach the commutative ellipsoid in the continuum limit $I \rightarrow \infty$.

7.2 Comparison to the fuzzy ellipsoid

As a final topic, we investigate the difference between the fuzzy ellipsoid and the ellipsoidal matrix geometry. The fuzzy ellipsoid is defined so as to satisfy

$$X^2 + Y^2 + \frac{1}{\mu^2} Z^2 = r^2 \mathbf{1}_I \quad \left(r := \sqrt{\frac{I-1}{I+1}} \right). \quad (7.4)$$

¹⁵(7.3) is reduced to (7.2) at $\mu = 1$.

$$\alpha(I-1)|_{\mu=1} = i \sum_{m>0}^{(I-1)/2} \frac{([X, Y])_{mm}}{(Z)_{mm}} = \frac{2}{I+1}. \quad (7.2)$$

The matrix coordinates for the fuzzy ellipsoid (7.4) are simply realized as

$$X = \alpha S_x^{(\frac{I}{2}-\frac{1}{2})}, \quad Y = \alpha S_y^{(\frac{I}{2}-\frac{1}{2})}, \quad Z = \mu \alpha S_z^{(\frac{I}{2}-\frac{1}{2})} \quad (\alpha := \frac{2}{I+1}), \quad (7.5)$$

which satisfy

$$[X, Y] = i\alpha \frac{1}{\mu} Z, \quad [Y, Z] = i\alpha \mu X, \quad [Z, X] = i\alpha \mu Y. \quad (7.6)$$

or the $SU(2)$ algebra

$$\left[\frac{X}{\alpha}, \frac{Y}{\alpha}\right] = i \frac{Z}{\mu \alpha}, \quad \left[\frac{Y}{\alpha}, \frac{Z}{\mu \alpha}\right] = i \frac{X}{\alpha}, \quad \left[\frac{Z}{\mu \alpha}, \frac{X}{\alpha}\right] = i \frac{Y}{\alpha}. \quad (7.7)$$

Equation (7.4) is invariant under the $SU(2)$ rotations generated by X , Y and $\frac{1}{\mu}Z$, which corresponds to the hidden $SU(2)$ symmetry of the classical ellipsoid (see Sec.4.2). Notice that the fuzzy ellipsoid algebra (7.6) is a linear algebra and it does not realize a quantum version of the classical non-linear algebra of ellipsoid (4.21). In Fig.16, we depict the evolution of the fuzzy ellipsoid with the normalized coordinates. Comparing Fig.16 with Fig.13, we can see that the evolution of the fuzzy ellipsoid is faster than that of the ellipsoidal matrix geometry.

Fuzzy ellipsoid

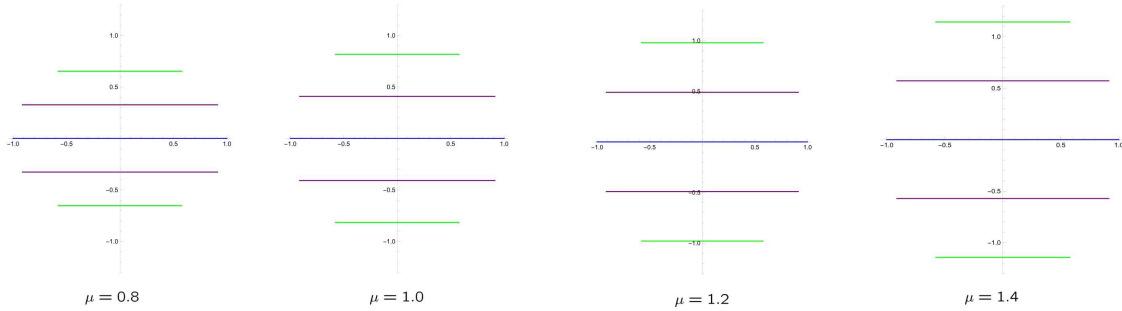


Figure 16: Evolution of the fuzzy ellipsoid of $I = 5$.

Recall that the ellipsoidal matrix geometries have the $U(1)$ symmetry, but not the $SU(2)$ symmetry, as the Landau Hamiltonian on ellipsoid only respects the $U(1)$ symmetry. Meanwhile, the fuzzy ellipsoid enjoys the $SU(2)$ symmetry as we have seen above. Since their symmetries are distinct, the fuzzy ellipsoids and the ellipsoidal matrix geometries are considered to describe different non-commutative geometries. In the following, we present a quantitative argument about the difference between the fuzzy ellipsoid and the zeroth Landau level matrix geometry. We first evaluate the Hilbert-Schmidt distance between $X^2 + Y^2 + \frac{1}{\mu^2}Z^2$ and $r(I-1)^2 \mathbf{1}_I$:

$$L_1 = \text{tr} \left(\sqrt{\left(X^2 + Y^2 + \frac{1}{\mu^2} Z^2 - r(I-1)^2 \mathbf{1}_I \right)^2} \right), \quad (7.8)$$

where $r(I-1)$ is given by (7.1). If X_i were the coordinates on the fuzzy ellipsoid, the quantity inside the trace of (7.8) would become zero. We then adopt the L_1 as an index of the discrepancy of the ellipsoidal matrix geometry from the fuzzy ellipsoid. The behavior of L_1 is depicted in the left of Fig.17. We also evaluate the following quantity

$$L_2 = \text{tr} \left(\sqrt{(\hat{X} - \hat{X}')^2 + (\hat{Y} - \hat{Y}')^2 + \frac{1}{\mu^2} (\hat{Z} - \hat{Z}')^2} \right), \quad (7.9)$$

where \hat{X}_i and \hat{X}'_i signify the normalized coordinates of the ellipsoidal matrix geometry and those the fuzzy ellipsoid, respectively. To reduce the overall scaling, we use the normalized matrix coordinates (5.18). The behavior of the L_2 is illustrated in the right of Fig.17. The numerical results show that the ellipsoidal matrix geometries do not coincide with the fuzzy ellipsoids and the discrepancies even grow as μ and I increase.

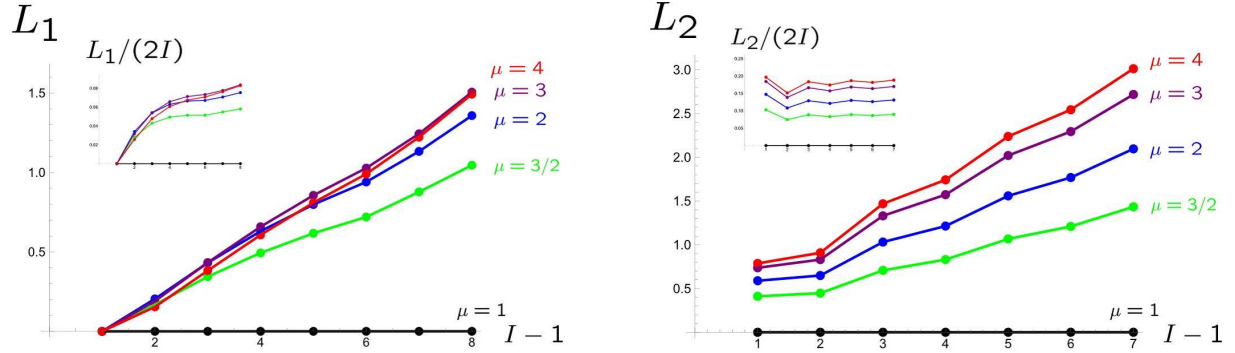


Figure 17: Left: The behavior of L_1 (7.8). Right: The behavior of L_2 (7.9). At $\mu = 1$, the ellipsoidal matrix geometry is reduced to the fuzzy sphere, so L_1 and L_2 are identically zeros. For $\mu \neq 1$, L_1 and L_2 generally grow as I and μ increase. (Subsets) The behaviors of the matrix distances normalized by $2I$. While the rates of increase of the distances become milder, the data imply that there still exist non-vanishing distances between the ellipsoidal matrix geometries and the fuzzy ellipsoids even in the continuum limit $I \rightarrow \infty$.

8 Summary

The construction of quantum matrix geometry for non-symmetric manifolds is crucial for further developments of non-commutative geometry. In this paper, we proposed a new scheme for the construction based on the spectral flow, which naturally embodies the concept of the (time-)evolution of matrix geometry. This scheme has the following properties (i) derivation of matrix coordinates is straightforward (ii) non-perturbative deformation is available (iii) unitarity is preserved. We applied this method to derive the matrix geometries of the expanding sphere and ellipsoid using the non-relativistic and relativistic Landau models. The magnetic field is taken to be compatible with the geometry of the base-manifold. We also numerically confirmed the Atiyah-Singer index theorem during the deformation from sphere to ellipsoid. The obtained ellipsoidal matrix geometries show qualitatively similar behaviors to the evolution of the original classical ellipsoid. The ellipsoidal matrix geometry evolves in a unique way in each Landau level. We checked that the ellipsoidal matrix geometries are consistently reduced to the corresponding classical ellipsoid in the commutative limit. We also numerically observed that the difference between the ellipsoidal matrix geometry and the fuzzy ellipsoid remains finite in the continuum limit.

Since this method is versatile, we can apply it to various manifolds including higher dimensional manifolds and topologically non-trivial manifolds. It may be interesting to consider a realistic non-commutative model for the time evolution of the universe. It is also worthwhile to see how the topological change of non-commutative spaces can be described in the present setup. According to the Atiyah-Singer index theorem, the topology change of a manifold necessarily induces the change of the number of associated zero modes, which leads to the change of the size of the matrix coordinates. The topological change is thus necessarily related to the violation of the unitarity of the non-commutative space. While the present approach is advantageous for deriving an explicit realization of the matrix coordinates, the underlying non-commutative

algebra is difficult to specify. This issue should be addressed in future research.

Acknowledgments

The author would like to thank Goro Ishiki, Kentaro Sato, Naoki Sasakura and Asato Tsuchiya for fruitful discussions and Akifumi Sako for helpful email correspondence. I am also very grateful to Professor Shuang Zhang for his warm hospitality at the University of Hong Kong. This work was supported by JSPS KAKENHI Grant No. 21K03542.

A Riemannian geometry of ellipsoid

We parameterize the ellipsoid

$$x^2 + y^2 + \left(\frac{z}{\mu}\right)^2 = 1, \quad (\text{A.1})$$

as

$$x = \sin \theta \cos \phi, \quad y = \sin \theta \sin \phi, \quad z = \mu \cos \theta, \quad (\text{A.2})$$

where $\theta = [0, \pi]$ and $\phi = [0, 2\pi)$. From the formula of the world line $ds^2 = \left(\frac{\partial \mathbf{x}}{\partial \theta} d\theta + \frac{\partial \mathbf{x}}{\partial \phi} d\phi\right)^2$, the non-zero components of the metric are derived as

$$g_{\theta\theta} = \rho^2, \quad g_{\phi\phi} = \sin^2 \theta, \quad (\text{A.3})$$

where

$$\rho = \sqrt{\cos^2 \theta + \mu^2 \sin^2 \theta}. \quad (\text{A.4})$$

The zweibein is derived as

$$e_1 = \rho d\theta, \quad e_2 = \sin \theta d\phi, \quad (\text{A.5})$$

and the spin-connection ω_{12} ($de_m + \sum_{n=1}^2 \omega_{mn} e_n = 0$) is

$$\omega_{12} = -\omega_{21} = -\frac{1}{\rho} \cos \theta d\phi. \quad (\text{A.6})$$

The corresponding curvature 2-form is obtained as

$$R_{12} = d\omega_{12} = \mu^2 \frac{\sin \theta}{\rho^3} d\theta \wedge d\phi, \quad (\text{A.7})$$

and its integral becomes

$$\int R_{12} = 4\pi. \quad (\text{A.8})$$

Using the metric (A.3), the area element of the ellipsoid is derived as

$$d\Omega = \sqrt{g} d\theta d\phi = \rho \sin \theta d\theta d\phi \quad (\text{A.9})$$

and the area of the ellipsoid $S = \int_{\text{ellipsoid}} d\Omega$ is calculated as

$$\mu > 1 \text{ (prolate spheroid)} \quad : \quad S = 2\pi \left(1 + \frac{\mu^2}{\sqrt{\mu^2 - 1}} \text{Arcsec}(\mu) \right), \quad (\text{A.10a})$$

$$\mu = 1 \text{ (sphere)} \quad : \quad S = 4\pi, \quad (\text{A.10b})$$

$$\mu < 1 \text{ (oblate spheroid)} \quad : \quad S = 2\pi \left(1 + \frac{\mu^2}{\sqrt{1 - \mu^2}} \text{Arcsech}(\mu) \right). \quad (\text{A.10c})$$

In the squashed-sphere-limit $\mu \rightarrow 0$, the oblate spheroid is completely flattened to be a double-sided unit disc with area π for each. Equation (A.10c) indeed yields $S \xrightarrow{\mu \rightarrow 0} 2 \times \pi$. The Gauss curvature K is derived as

$$K = \frac{1}{2} \mathcal{R} = \frac{\mu^2}{\rho^4}, \quad (\text{A.11})$$

which is related to the curvature two-form (A.7) by

$$R_{12} = e_1 \wedge e_2 K. \quad (\text{A.12})$$

The Euler number is evaluated as

$$\chi = \frac{1}{2\pi} \int d\theta d\phi \sqrt{g} K = \frac{1}{2\pi} \int R_{12} = 2. \quad (\text{A.13})$$

B Free particle on an ellipsoid

For completeness, we present the spectral flow of the free particle quantum mechanics on ellipsoid.

B.1 Non-relativistic free particle on an ellipsoid

The Schrödinger equation on ellipsoid is given by¹⁶

$$H_0 = -\frac{1}{2M} \frac{1}{\sqrt{g}} \partial_\mu (\sqrt{g} g^{\mu\nu} \partial_\nu) = -\frac{1}{2M} \left(\frac{1}{\rho^2} \partial_\theta^2 + \cot \theta \frac{1}{\rho^4} \partial_\theta + \frac{1}{\sin^2 \theta} \partial_\phi^2 \right), \quad (\text{B.2})$$

where $g_{\mu\nu}$ denote the metric on the ellipsoid (A.3) and

$$\rho := \sqrt{\mu^2(x^2 + y^2) + \frac{1}{\mu^2} z^2} = \sqrt{\cos^2 \theta + \mu^2 \sin^2 \theta}. \quad (\text{B.3})$$

The quantum mechanical Hamiltonian (B.2) does not have the $SU(2)$ symmetry (except for $\mu = 1$), but only has the $U(1)$ symmetry generated by L_z :

$$[H_0, L_z] = 0. \quad (\text{B.4})$$

Obviously, the lowest energy of H_0 is zero for any value of μ and the lowest energy state is given by the constant wavefunction:

$$\varphi = \frac{1}{\sqrt{S}}, \quad (\text{B.5})$$

where S is the area of the ellipsoid (A.10). The constant wavefunction (B.5) corresponds to the s -wave spherical harmonics in the spherical system. The spectral flow of H_0 is depicted in Fig.18.

B.2 Relativistic free particle on an ellipsoid

The square of the free Dirac operator is represented by the following Lichnerowicz formula

$$(-i\nabla)^2 = -\Delta + \frac{\mathcal{R}}{4}, \quad (\text{B.6})$$

¹⁶At the disc limit $\mu \rightarrow 0$, (B.2) is reduced to the polar coordinate Hamiltonian on a disc,

$$H_0 \rightarrow -\frac{1}{2M} \left(\frac{\partial^2}{\partial \tilde{r}^2} + \frac{1}{\tilde{r}} \frac{\partial}{\partial \tilde{r}} + \frac{1}{\tilde{r}^2} \frac{\partial^2}{\partial \phi^2} \right), \quad (\text{B.1})$$

where $\tilde{r} := \sin \theta$.

Non-relativistic case (free particle)

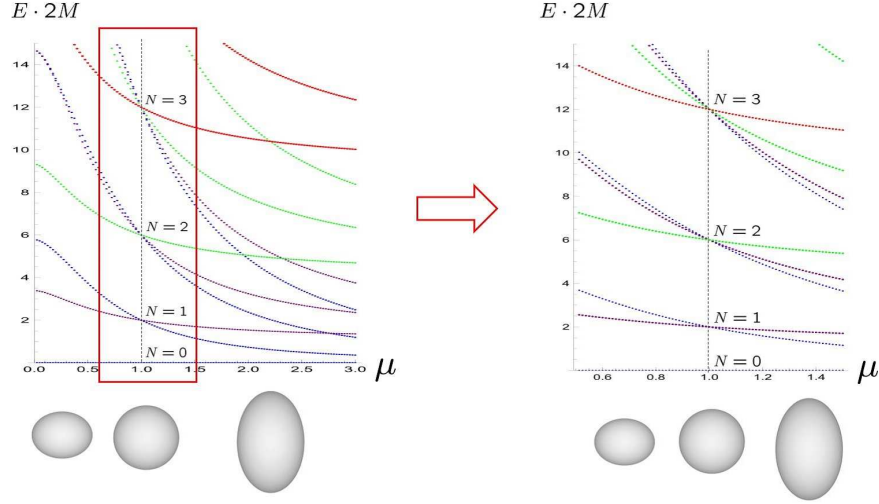


Figure 18: The spectral flow of the eigenvalues of (B.2). At $\mu = 1$ (sphere), the Hamiltonian has $SU(2)$ symmetry and its eigenvalues are given by $N(N + 1)$ ($N = 0, 1, 2, \dots$) with degeneracy $2N + 1$ and the corresponding eigenstates are the spherical harmonics. The $m = 0, \pm 1, \pm 2, \pm 3$ states correspond to the blue, violet, green and red curves, respectively. The lowest energy remains at zero for arbitrary μ .

where $\mathcal{R} = 2\frac{\mu^2}{\rho^4}$ denotes the scalar curvature and Δ signifies a Laplace-Beltrami operator,

$$\Delta := \frac{1}{\sqrt{g}} \nabla_\mu (\sqrt{g} g^{\mu\nu} \nabla_\nu). \quad (\text{B.7})$$

With the spin connection (A.6), the covariant derives, $\nabla_\mu := \partial_\mu + i\omega_\mu$, are given by

$$\nabla_\theta = \partial_\theta, \quad \nabla_\phi = \partial_\phi + i\omega_\phi = \partial_\phi - i\frac{1}{2\rho} \cos\theta \sigma_3, \quad (\text{B.8})$$

and (B.6) is expressed as

$$(-i\nabla)^2 = -\frac{1}{\rho^2} \partial_\theta^2 - \cot\theta \frac{1}{\rho^4} \partial_\theta - \frac{1}{\sin^2\theta} \nabla_\phi^2 + \frac{1}{2} \frac{\mu^2}{\rho^4}. \quad (\text{B.9})$$

For $\mu = 1$, (B.9) is reduced to

$$(-i\nabla)^2|_{\mu=1} = -\partial_\theta^2 - \cot\theta \partial_\theta - \frac{1}{\sin^2\theta} \left(\partial_\phi - i\frac{1}{2} \cos\theta \sigma_3 \right)^2 + \frac{1}{2}. \quad (\text{B.10})$$

The spectral flow of (B.9) is depicted in Fig.19.

References

- [1] Michael R. Douglas, Nikita A. Nekrasov, “*Noncommutative Field Theory*”, Rev.Mod.Phys.73 (2001) 977-1029, hep-th/0106048.
- [2] Washington Taylor, “*Lectures on D-branes, Gauge Theory and M(atrices)*”, hep-th/9801182.

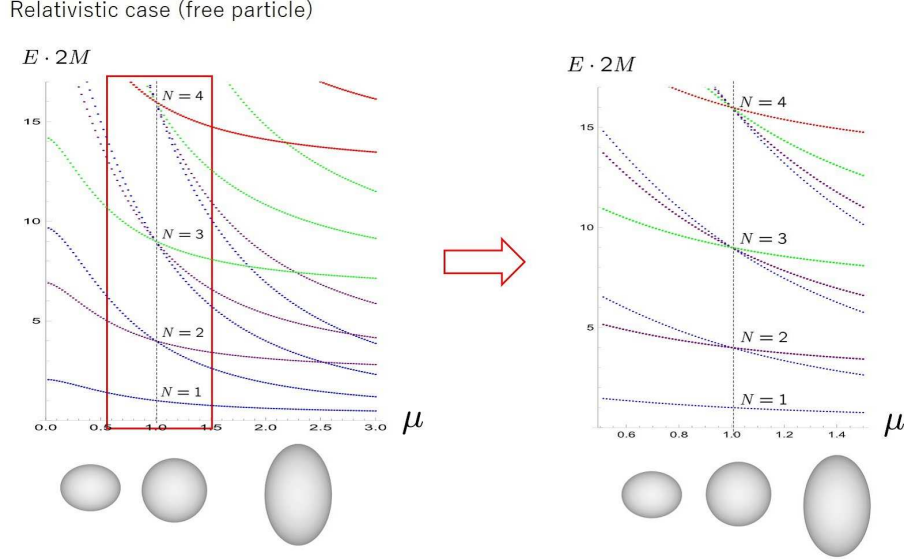


Figure 19: The spectral flow of the eigenvalues of (B.9). At $\mu = 1$ (sphere), the square of the Dirac operator has the eigenvalues N^2 ($N = 1, 2, 3, \dots$) with $4N$ -fold degeneracy. The $m = \pm 1/2, \pm 3/2, \pm 5/2, \pm 7/2$ states with spin degrees of freedom correspond to the blue, violet, green and red curves, respectively.

- [3] Dimitra Karabali, V.P. Nair, S. Randjbar-Daemi “*Fuzzy spaces, the M(atrrix) model and the quantum Hall effect*”, hep-th/0407007.
- [4] Kazuki Hasebe, “*Hopf Maps, Lowest Landau Level, and Fuzzy Spheres*”, SIGMA 6 (2010) 071; arXiv:1009.1192.
- [5] Pei-Ming Ho, Yutaka Matsuo, “*Nambu bracket and M-theory*”, Prog. Theo. Exp. Phys. (2016) 06A104; arXiv:1603.09534.
- [6] S.M. Girvin, Terrence Jach, “*Formalism for the quantum Hall effect: Hilbert space of analytic functions*”, Phys. Rev. B 29 (1984) 5617-5625.
- [7] Z.F. Ezawa, G. Tsitshishvili, K. Hasebe, “*Noncommutative geometry, extended W_∞ algebra, and Grassmannian solitons in multicomponent quantum Hall systems*”, Phys. Rev. B 67 (2003) 125314.
- [8] Kazuki Hasebe, “*Supersymmetric Quantum Hall Effect on a Fuzzy Supersphere*”, Phys.Rev.Lett. 94 (2005) 206802; hep-th/0411137.
- [9] Titus Neupert, Luiz Santos, Shinsei Ryu, Claudio Chamon, Christopher Mudry, “*Noncommutative geometry for three-dimensional topological insulators*”, Phys. Rev. B 86 (2012) 035125; arXiv:1202.5188.
- [10] B. Estienne, N. Regnault, B. A. Bernevig, “*D-Algebra Structure of Topological Insulators*”, Phys. Rev. B 86 (2012) 241104(R); arXiv:1202.5543.
- [11] Ken Shiozaki, Satoshi Fujimoto, “*Electromagnetic and thermal responses of Z topological insulators and superconductors in odd spatial dimensions*”, Phys. Rev. Lett. 110 (2013) 076804; arXiv:1210.2825.
- [12] Kazuki Hasebe, “*Higher Dimensional Quantum Hall Effect as A-Class Topological Insulator*”, Nucl.Phys. B 886 (2014) 952-1002; arXiv:1403.5066.

- [13] Kazuki Hasebe, “*Chiral topological insulator on Nambu 3-algebraic geometry*”, Nucl.Phys. B 886 (2014) 681-690; arXiv:1403.7816.
- [14] Kazuki Hasebe, “*Higher (Odd) Dimensional Quantum Hall Effect and Extended Dimensional Hierarchy*”, Nucl.Phys. B 920 (2017) 475-520; arXiv:1612.05853.
- [15] Edwin Langmann, Shinsei Ryu, Ken Shiozaki, “*Higher bracket structure of density operators in Weyl fermion systems and topological insulators*”, arXiv:2401.09683.
- [16] Kazuki Hasebe, “*Perfectly spherical Bloch hyper-spheres from quantum matrix geometry*”, Nucl. Phys. B 1005 (2024) 116595; arXiv:2402.07149.
- [17] Päivi Törmä, “*Essay: Where Can Quantum Geometry Lead Us?*”, Phys. Rev. Lett. 131 (2023) 240001; arXiv:2312.11516.
- [18] Wei Zhu, Chao Han, Emilie Huffman, Johannes S. Hofmann, and Yin-Chen He, “*Uncovering Conformal Symmetry in the 3D Ising Transition: State-Operator Correspondence from a Quantum Fuzzy Sphere Regularization*”, Phys.Rev. X 13 (2023) 021009; arXiv:2210.13482.
- [19] Gabriel Cuomo, Zohar Komargodski, Márk Mezei, Avia Raviv-Moshe, “*Spin Impurities, Wilson Lines and Semiclassics*”, JHEP 06 (2022) 112; arXiv:2202.00040.
- [20] Gabriel Cuomo, Anton de la Fuente, Alexander Monin, David Pirtskhalava, Riccardo Rattazzi, “*Rotating superfluids and spinning charged operators in conformal field theory*”, Phys.Rev. D 97 (2018) 045012; arXiv:1711.02108.
- [21] Gabriel Cuomo, Luca V. Delacretaz, Umang Mehta, “*Large Charge Sector of 3d Parity-Violating CFTs*”, JHEP 05 (2021) 115; arXiv:
- [22] Jens Hoppe, “*Quantum Theory of a Massless Relativistic Surface and a Two-dimensional Bound State Problem*”, MIT PhD Thesis (1982).
- [23] J. Madore, “*The Fuzzy Sphere*”, Class. Quant. Grav. 9 (1992) 69.
- [24] G.Alexanian, A.P.Balachandran, G.Immirzi, B.Ydri, “*Fuzzy CP²*”, J.Geom.Phys.42 (2002) 28-53; hep-th/0103023.
- [25] A.P. Balachandran, Brian P. Dolan, J. Lee, X. Martin, Denjoe O’Connor, “*Fuzzy Complex Projective Spaces and their Star-products*”, J.Geom.Phys. 43 (2002) 184-204; hep-th/0107099.
- [26] H. Grosse, C. Klimcik, P. Presnajder, “*On Finite 4D Quantum Field Theory in Non-Commutative Geometry*”, Commun.Math.Phys. 180 (1996) 429-438; hep-th/9602115.
- [27] Judith Castelino, Sangmin Lee, Washington Taylor, “*Longitudinal 5-branes as 4-spheres in Matrix theory*”, Nucl.Phys.B526 (1998) 334-350; hep-th/9712105.
- [28] P. M. Ho and S. Ramgoolam, “*Higher dimensional geometries from matrix brane constructions*”, Nucl.Phys.B 627 (2002) 266; hep-th/0111278.
- [29] Sanjaye Ramgoolam, “*Higher dimensional geometries related to fuzzy odd-dimensional spheres*”, JHEP 0210 (2002) 064; hep-th/0207111.
- [30] Pei-Ming Ho, Miao Li, “*Large N Expansion From Fuzzy AdS²*”, Nucl.Phys. B590 (2000) 198-212; hep-th/0005268.

- [31] Kazuki Hasebe, “*Non-Compact Hopf Maps and Fuzzy Ultra-Hyperboloids*”, Nucl.Phys. B 865 (2012) 148-199; arXiv:1207.1968.
- [32] H. Grosse, C. Klimcik and P. Presnajder, “*Field Theory on a Supersymmetric Lattice*”, Comm.Math.Phys. 185 (1997) 155, hep-th/9507074.
- [33] H. Grosse and G. Reiter, “*The Fuzzy Supersphere*”, Jour. Geom. Phys. 28 (1998) 349, math-ph/9804013.
- [34] Kazuki Hasebe, “*Graded Hopf maps and fuzzy super-spheres*”, Nucl.Phys. B 853 (2011) 777; arXiv:1106.5077.
- [35] Dimitra Karabali, V.P. Nair, “*Quantum Hall Effect in Higher Dimensions*”, Nucl.Phys. B641 (2002) 533-546; hep-th/0203264.
- [36] Dimitra Karabali, V.P. Nair, “*Quantum Hall Effect in Higher Dimensions, Matrix Models and Fuzzy Geometry*”, J.Phys.A39 (2006) 12735-12764; hep-th/0606161.
- [37] Kazuki Hasebe, “*Relativistic Landau Models and Generation of Fuzzy Spheres*”, Int.J.Mod.Phys.A 31 (2016) 1650117; arXiv:1511.04681.
- [38] V.P. Nair, S. Randjbar-Daemi, “*Quantum Hall effect on S^3 , edge states and fuzzy S^3/\mathbf{Z}_2* ”, Nucl.Phys. B679 (2004) 447-463; hep-th/0309212.
- [39] Kazuki Hasebe, “*SO(4) Landau Models and Matrix Geometry*”, Nucl.Phys. B 934 (2018) 149-211; arXiv:1712.07767.
- [40] S. C. Zhang and J. P. Hu, “*A Four Dimensional Generalization of the Quantum Hall Effect*”, Science 294 (2001) 823; cond-mat/01110572.
- [41] Kazuki Hasebe, Yusuke Kimura, “*Dimensional Hierarchy in Quantum Hall Effects on Fuzzy Spheres*”, Phys.Lett. B602 (2004) 255-260; hep-th/0310274.
- [42] G. Ishiki, T. Matsumoto, H. Muraki, “*Information metric, Berry connection, and Berezin-Toeplitz quantization for matrix geometry*”, Phys. Rev. D 98 (2018) 026002; arXiv:1804.00900.
- [43] Kazuki Hasebe, “*SO(5) Landau models and nested Nambu matrix geometry*”, Nucl.Phys. B 956 (2020) 115012; arXiv:2002.05010.
- [44] Kazuki Hasebe, “*SO(5) Landau model and 4D quantum Hall effect in the SO(4) monopole background*”, Phys.Rev. D 105 (2022) 065010; arXiv:2112.03038 .
- [45] Kazuki Hasebe, “*Generating Quantum Matrix Geometry from Gauge Quantum Mechanics*”, Phys. Rev. D 108 (2023) 126023; arXiv:2310.01051.
- [46] Kazuki Hasebe, Yusuke Kimura, “*Fuzzy Supersphere and Supermonopole*”, Nucl.Phys.B709 (2005) 94-114; hep-th/0409230.
- [47] Evgeny Ivanov, Luca Mezincescu, Paul K. Townsend, “*Fuzzy CP(n|m) as a quantum superspace*”, hep-th/0311159.
- [48] Hiroyuki Adachi, Goro Ishiki, Takaki Matsumoto, Kaishu Saito, “*The matrix regularization for Riemann surfaces with magnetic fluxes*”, Phys. Rev. D 101 (2020) 106009; arXiv:2002.02993.

- [49] Hiroyuki Adachi, Goro Ishiki, Satoshi Kanno, “*Vector bundles on fuzzy Kähler manifolds*”, Prog. Theor. Exp. Phys. (2023) 023B01; arXiv:2210.01397.
- [50] Joakim Arnlind, Martin Bordemann, Laurent Hofer, Jens Hoppe, Hidehiko Shimada, “*Noncommutative Riemann Surfaces by Embeddings in \mathbb{R}^3* ”, Commun.Math.Phys. 288 (2009) 403-429 ; arXiv:0711.2588.
- [51] Joakim Arnlind, Martin Bordemann, Laurent Hofer, Jens Hoppe, Hidehiko Shimada, “*Fuzzy Riemann surfaces*”, JHEP 06 (2009) 047; hep-th/0602290.
- [52] S. Klimek, A. Lesniewski, “*Quantum Riemann surfaces I. The unit disc*”, Commun.Math.Phys. 146 (1992) 103-122.
- [53] S. Klimek, A. Lesniewski, “*Quantum Riemann surfaces II. The discrete series*”, Lett.Math.Phys. 24 (1992) 125-139.
- [54] Martin Bordemann, Eckhard Meinrenken, Martin Schlichenmaier, “*Toeplitz Quantization of Kähler Manifolds and $gl(N)N \rightarrow \infty$* ”, Commun.Math.Phys. 165 (1994) 281-296; hep-th/9309134.
- [55] Xiaonan Ma, George Marinescu, “*Toeplitz operators on symplectic manifolds*”, J. Geom. Anal 18 (2008) 565; arXiv:0806.2370.
- [56] Naoki Sasakura, “*Non-unitary evolutions of noncommutative worlds with symmetry*”, JHEP 0401 (2004) 016; arXiv:hep-th/0309035.
- [57] Naoki Sasakura, “*Evolving fuzzy CP^n and lattice n -simplex*”, Phys.Lett. B599 (2004) 319-325; hep-th/0406167.
- [58] Mitsuaki Hirasawa, Konstantinos N. Anagnostopoulos, Takehiro Azuma, Kohta Hatakeyama, Jun Nishimura, Stratos Papadoudis, Asato Tsuchiya, “*The effects of SUSY on the emergent spacetime in the Lorentzian type IIB matrix model*”, proceedings of Corfu Summer Institute 2023 ”School and Workshops on Elementary Particle Physics and Gravity”; arXiv:2407.03491.
- [59] Kohta Hatakeyama, Akira Matsumoto, Jun Nishimura, Asato Tsuchiya, Atis Yosprakob, “*The emergence of expanding space-time and intersecting D-branes from classical solutions in the Lorentzian type IIB matrix model*”, Prog. Theor. Exp. Phys. (2020) 043B10; arXiv:1911.08132.
- [60] Harold C. Steinacker, “*Cosmological space-times with resolved Big Bang in Yang-Mills matrix models*”, JHEP 02 (2018) 033; arXiv:1709.10480.
- [61] Harold C. Steinacker, “*Quantized open FRW cosmology from Yang-Mills matrix models*”, Phys. Lett. B 782 (2018) 176; arXiv:1710.11495.
- [62] A. Stern, Chuang Xu, “*Signature change in matrix model solutions*”, Phys. Rev. D 98 (2018) 086015; arXiv:1808.07963.
- [63] V. P. Nair, “*Landau-Hall states and Berezin-Toeplitz quantization of matrix algebras*”, Phys.Rev. D 102 (2020) 025015; arXiv:2001.05040.
- [64] Goro Ishiki, Takaki Matsumoto, Hisayoshi Muraki, “*Kähler structure in the commutative limit of matrix geometry*”, JHEP 08 (2016) 042; arXiv:1603.09146.
- [65] Kaho Matsuura, Asato Tsuchiya, “*Matrix geometry for ellipsoids*”, Prog. Theor. Exp. Phys. (2020) 033B05.

- [66] T.T. Wu, C.N. Yang, “*Dirac Monopoles without Strings: Monopole Harmonics*”, Nucl.Phys. B107 (1976) 365-380.
- [67] F.D.M. Haldane, “*Fractional quantization of the Hall effect: a hierarchy of incompressible quantum fluid states*”, Phys. Rev. Lett. 51 (1983) 605-608.
- [68] Stefan Andronache, Harold C. Steinacker, “*The squashed fuzzy sphere, fuzzy strings and the Landau problem*”, J. Phys. A: Math. Theor. 48 (2015) 295401; arXiv:1503.03625.
- [69] George Dassios, “*Ellipsoidal Harmonics*”, Cambridge University Press (2012).
- [70] Brian P. Dolan, “*The Spectrum of the Dirac Operator on Coset Spaces with Homogeneous Gauge Fields*”, JHEP 0305 (2003) 018; hep-th/0302122.